

# NAVAL POSTGRADUATE SCHOOL Monterey, California



## THESIS

**PERFORMANCE OF FFH/BFSK SYSTEMS WITH CONVO-  
LUTIONAL CODING AND SOFT DECISION VITERBI DE-  
CODING OVER Rician FADING CHANNELS WITH  
PARTIAL-BAND NOISE INTERFERENCE**

by

Michael D. Theodoss

December 1995

Thesis Advisor:

R. Clark Robertson

Approved for public release; distribution is unlimited.

19960327 072

19960327 072

# REPORT DOCUMENTATION PAGE

*Form Approved*  
OMB No. 0704-0188

Public reporting burden for this collection of information is estimated to average 1 hour per response, including the time reviewing instructions, searching existing data sources gathering and maintaining the data needed, and completing and reviewing the collection of information. Send comments regarding this burden estimate or any other aspect of this collection of information, including suggestions for reducing this burden to Washington Headquarters Services, Directorate for Information Operations and Reports, 1215 Jefferson Davis Highway, Suite 1204, Arlington, VA 22202-4302, and to the Office of Management and Budget, Paperwork Reduction Project (0704-0188), Washington, DC 20503.

<b>1. AGENCY USE ONLY (Leave Blank)</b>		<b>2. REPORT DATE</b> December 1995	<b>3. REPORT TYPE AND DATES COVERED</b> Master's Thesis	
<b>4. TITLE AND SUBTITLE</b> PERFORMANCE OF FFH/BFSK SYSTEMS WITH CONVOLUTIONAL CODING AND SOFT DECISION VITERBI DECODING OVER RICIAN FADING CHANNELS WITH PARTIAL-BAND NOISE INTERFERENCE (U)			<b>5. FUNDING NUMBERS</b>	
<b>6. AUTHOR(S)</b> Theodoss, Michael D.				
<b>7. PERFORMING ORGANIZATION NAME(S) AND ADDRESS(ES)</b> Naval Postgraduate School Monterey, CA 93943-5000			<b>8. PERFORMING ORGANIZATION REPORT NUMBER</b>	
<b>9. SPONSORING/ MONITORING AGENCY NAME(S) AND ADDRESS(ES)</b>			<b>10. SPONSORING/ MONITORING AGENCY REPORT NUMBER</b>	
<b>11. SUPPLEMENTARY NOTES</b> The views expressed in this thesis are those of the author and do not reflect the official policy or position of the Department of Defense or the United States Government.				
<b>12a. DISTRIBUTION / AVAILABILITY STATEMENT</b> Approved for public release; distribution is unlimited.			<b>12b. DISTRIBUTION CODE</b>	
<b>13. ABSTRACT (Maximum 200 words)</b> An error probability analysis of a communications link employing convolutional coding with soft decision Viterbi decoding implemented on a fast frequency-hopped, binary frequency-shift keying (FFH/BFSK) spread spectrum system is performed. The signal is transmitted through a Rician fading channel with partial-band noise interference. The receiver structures examined are the conventional receiver with no diversity, the conventional receiver with diversity and the assumption of perfect side information, and the self-normalized combining receiver with diversity. The self-normalized receiver minimizes the effects of hostile partial-band interference, while diversity alleviates the effects of fading. It is found that with the implementation of soft decision Viterbi decoding the performance of the self-normalized receiver is improved dramatically for moderate coded bit energy to partial-band noise power spectral density ratio ( $E_b/N_f$ ). Coding drives the jammer to a full band jamming strategy for worst case performance. Nearly worst case jamming occurs when barrage jamming is employed and there is no diversity even in cases where there is very strong direct signal. Performance improves as the constraint length of the convolutional code is increased. For the most powerful convolutional codes, performance is seen to degrade slightly with increasing diversity except in instances of a very weak direct signal. Also, soft decision decoding is found to be superior to hard decision decoding by approximately 4 dB at moderate $E_b/N_f$ .				
<b>14. SUBJECT TERMS</b> fast frequency-hopping, self-normalization, convolutional coding			<b>15. NUMBER OF PAGES</b> 80	
			<b>16. PRICE CODE</b>	
<b>17. SECURITY CLASSIFICATION OF REPORT</b> Unclassified	<b>18. SECURITY CLASSIFICATION OF THIS PAGE</b> Unclassified	<b>19. SECURITY CLASSIFICATION OF ABSTRACT</b> Unclassified	<b>20. LIMITATION OF ABSTRACT</b> UL	



Approved for public release; distribution is unlimited

**PERFORMANCE OF FFH/BFSK SYSTEMS WITH CONVOLUTIONAL CODING AND SOFT DECISION VITERBI DECODING OVER Rician FADING CHANNELS WITH PARTIAL-BAND NOISE INTERFERENCE**

Michael D. Theodoss  
Captain, United States Army  
B.S.E.E., University of Massachusetts at Amherst, 1987

Submitted in partial fulfillment of the  
requirements for the degree of

**MASTER OF SCIENCE IN ELECTRICAL ENGINEERING**

from the

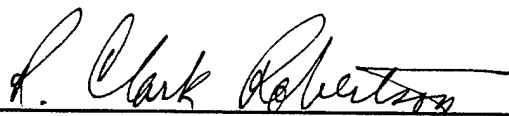
**NAVAL POSTGRADUATE SCHOOL  
December 1995**

Author:

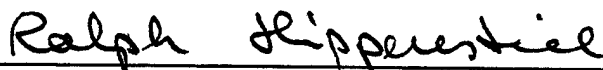


Michael D. Theodoss

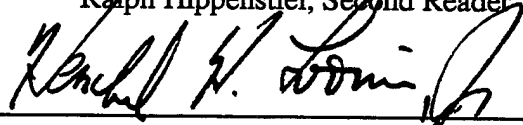
Approved by:



R. Clark Robertson, Thesis Advisor



Ralph Hippenstiel, Second Reader



Herschel H. Loomis, Jr., Chairman,  
Department of Electrical and Computer Engineering



## ABSTRACT

An error probability analysis of a communications link employing convolutional coding with soft decision Viterbi decoding implemented on a fast frequency-hopped, binary frequency-shift keying (FFH/BFSK) spread spectrum system is performed. The signal is transmitted through a Rician fading channel with partial-band noise interference. The receiver structures examined are the conventional receiver with no diversity, the conventional receiver with diversity and the assumption of perfect side information, and the self-normalized combining receiver with diversity. The self-normalized receiver minimizes the effects of hostile partial-band interference, while diversity alleviates the effects of fading. It is found that with the implementation of soft decision Viterbi decoding that the performance of the self-normalized receiver is improved dramatically for moderate coded bit energy to partial-band noise power spectral density ratio ( $E_b/N_I$ ). Coding drives the jammer to a full band jamming strategy for worst case performance. Nearly worst case jamming occurs when barrage jamming is employed and there is no diversity even in cases where there is very strong direct signal. Performance improves as the constraint length of the convolutional code is increased. Performance is seen to degrade slightly with increasing diversity except in instances of a very weak direct signal. Also, soft decision decoding is found to be superior to hard decision decoding by approximately 4 dB at moderate  $E_b/N_I$ .



## TABLE OF CONTENTS

I. INTRODUCTION .....	1
II. OVERVIEW OF SYSTEMS .....	5
A. SPREAD SPECTRUM OVERVIEW .....	5
B. FREQUENCY-HOPPED SPREAD SPECTRUM .....	5
C. FAST FREQUENCY-HOPPED BINARY FREQUENCY-SHIFT KEYING (FFH/BFSK) .....	6
D. SOURCES OF PERFORMANCE DEGRADATION .....	10
1. Thermal Noise .....	10
2. Partial-Band Interference .....	10
3. Fading Multipath Channel .....	11
E. FORWARD ERROR CORRECTION .....	13
F. ENERGY AND BANDWIDTH CONSIDERATIONS .....	16
G. THE SELF-NORMALIZED RECEIVER .....	17
III. PERFORMANCE ANALYSIS FOR FFH/BFSK CONVENTIONAL RECEIVER WITH PERFECT SIDE INFORMATION AND CONVOLUTIONAL CODING ..	19
A. PERFORMANCE WITHOUT FADING .....	19
B. PERFORMANCE IN FADING CHANNELS .....	22
IV. PERFORMANCE ANALYSIS FOR FFH/BFSK SELF-NORMALIZED RECEIVER WITH CONVOLUTIONAL CODING .....	27
A. ANALYSIS .....	27
B. PROBABILITY OF BIT ERROR .....	29
V. NUMERICAL ANALYSIS .....	33
A. NUMERICAL PROCEDURE .....	33
1. Constant Bit Energy and Constant Spread Bandwidth .....	35
2. Constant Hop Energy and Varying Spread Bandwidth .....	36
3. Constant Bit Energy and Varying Spread Bandwidth Systems .....	36
VI. NUMERICAL RESULTS AND DISCUSSION .....	39

VII. CONCLUSION .....	63
LIST OF REFERENCES .....	67
INITIAL DISTRIBUTION LIST .....	69

## LIST OF SYMBOLS

$\Delta f$	Frequency separation
$\Delta f_{fh}$	Frequency separation between hopping bins
$\theta_{s_i}$	Signal phase
$\alpha^2$	Average power of the non-faded (direct) component of a signal
$2\sigma^2$	Average power of the Rayleigh-faded (diffuse) component of a signal
$\sigma_k^2$	Noise power per hop at the receiver output
$\eta$	Ratio of direct/diffuse signal power
$\rho_k$	$\alpha^2/\sigma_k^2$
$\xi_k$	$2\sigma^2/\sigma_k^2$
$\sqrt{2}a_k$	Received signal amplitude of signal corresponding to $k^{\text{th}}$ hop. Modeled as a Rician random variable.
AWGN	Additive white Gaussian noise.
B	Minimum equivalent noise bandwidth of receiver matched filters
BFSK	Binary frequency-shift keying
$d_{\text{free}}$	Hamming free distance
$E_b$	Uncoded bit energy
$E_h$	Hop energy
$E_s$	Symbol energy
$f_{\Sigma}(\Sigma)$	Probability distribution function of random variable $\Sigma$
FFH	Fast frequency-hopping
$I_{L-1}(\bullet)$	Modified Bessel function of the first kind and order L-1

$k$	Size of input codeword
$\mathcal{L}_m^{L-1}$	Laguerre polynomial
$L$	Diversity, hops/symbol
$n$	Size of output codeword
$N_I$	Power spectral density of the jamming noise
$N_o$	Power spectral density of the thermal noise
$N_T$	Power spectral density of the total noise
$p$	Probability distribution function
$P_b$	Probability of bit error
$P_s(i)$	Error probability given $i$ coded hops are jammed.
$P_2(d)$	Probability of error between two codewords of Hamming distance $d$
$r$	Code rate, $k/n$
$R_b$	Information bit rate
$R_h$	Hop rate
SNR	Signal-to-thermal noise power ratio
$T_h$	Hop duration
$T_s$	Symbol duration
$v$	Constraint length of a code
$w_d$	Total information weight of a path of weight $d$
$x_{1k}, x_{2k}$	Demodulator outputs at receiver branch 1 and 2
$z_{1k}, z_{2k}$	Normalized outputs at receiver branch 1 and 2

## I. INTRODUCTION

The purpose of this thesis is to investigate the performance of noncoherent fast frequency-hopped binary frequency-shift keying (FFH/BFSK) receivers under conditions of Rician fading and hostile partial-band noise interference. The data is assumed to be encoded using convolutional coding, and the receivers are assumed to use either soft or hard decision decoding. The receiver structures examined are the conventional receiver with no diversity, the conventional receiver with diversity and the assumption of perfect side information, and the self-normalized receiver with diversity. Without error correction coding or diversity, the performances of the conventional receiver with no side information, the conventional receiver with perfect side information and the self-normalized receiver are all equivalent. The performance of the conventional receiver with no diversity or coding provides a baseline against which to measure the advantages of diversity, coding, and side information. The assumption of perfect side information is unrealistic but provides an ideal against which the self-normalized receiver can be compared.

Fast frequency-hopping with diversity implies that multiple hops representing a bit are transmitted at different carrier frequencies known only to the transmitter and receiver. Fast frequency-hopped systems are susceptible to partial-band interference when the demodulator assigns equal weight to each of the diversity receptions representing a bit [Ref. 1]. When the hops are combined in this manner to form the decision statistic, the receiver is called a linear combining receiver. Previous works have examined methods to mitigate the effects of partial-band jamming on a FFH/BFSK system. For a diversity system, one technique to combat the partial-band jammer is for the demodulator to have information available allowing it to give less weight to those received hops with jamming present than hops with no interference present. Such information is called side information. A demodulator which has the capability of neglecting all jammed hops and using only unjammed hops has perfect side information. Since such a demodulator requires

knowledge of the jammer state which is not generally available in practice, other techniques to provide some type of side information have been developed. The analysis of the receiver with perfect side information and no thermal noise does provide a lower bound on probability of bit error against which to measure the performance of other more realistic systems.

Nonlinear combining receivers assign different weights to diversity receptions representing a bit. Nonlinear combining receivers with diversity are superior to linear combining receivers in combatting partial-band jamming provided that the signal-to-thermal noise power ratio (SNR) is high enough such that noncoherent combining losses do not dominate over the reduction in jamming effectiveness provided by the weighting strategy [Ref. 2]. A specific type of nonlinear combining receiver is the noise-normalized or adaptive gain control (AGC) receiver. The noise-normalized receiver measures the noise power present in each hop and then uses the reciprocal of this measurement to normalize the output of each detector branch before the diversity hop receptions are combined. For such a system, the hops with jamming present are deemphasized. Such a system was examined by Lee, French, and Miller [Ref. 2] for nonfading channels and by Robertson and Ha [Ref. 3] for Rician fading channels. The noise-normalized receiver was shown to neutralize the effects of partial-band jamming when the diversity of the system is sufficiently large.

The self-normalized receiver is another type of nonlinear combining receiver. The receiver is called self-normalized because there is no measurement of signal or noise powers as required in the noise-normalized receiver. Instead the self-normalized receiver uses the detected hops themselves to derive weights or normalization factors [Ref. 4]. The self-normalized receiver will be described in Chapter II and its performance with convolutional coding analyzed in Chapter IV. Previous works have shown that the self-normalized receiver with diversity neutralized performance degradation due to partial-band noise jamming. The performance of the receiver improves with diversity when fading is present provided that the SNR is above 13dB [Ref. 5].

The use of forward error correction techniques are another effective method to mitigate the effects of partial-band jamming [Ref. 6]. A repetition code is a forward error correction code which is equivalent to diversity transmission of the information bits. A system with perfect side information and soft decisions using repetition coding minimizes the effectiveness of partial-band jamming. The jammer is forced to transmit over a wider bandwidth and is driven towards full band jamming which is the most benign [Ref. 7]. Codes more powerful than repetition codes can further improve performance and allow for reliable communications. One such code is a convolutional code. Neglecting thermal noise, Stark [Ref. 8] evaluated the performance of a conventional frequency-hopped BFSK receiver with no diversity in the presence of worst case partial-band jamming. With a bit error probability of  $10^{-5}$ , his results showed a coding gain of about 29 dB through the use of rate 1/2 and constraint length 7 convolutional codes with hard decisions and no side information available. The use of side information improved performance by another 5 dB and the use of soft decisions over hard decisions gave approximately an additional 2 dB improvement.

The combination of nonlinear combining techniques and convolutional coding further diminish the effectiveness of partial-band jamming. The noise-normalized receiver with coding has been shown to provide a large improvement over uncoded performance for FFH/BFSK [Ref. 9] as well as for the more general fast frequency-hopped M-ary frequency shift keying (FFH/MFSK) receiver [Ref. 3]. The performance of the self-normalized receiver is expected to be similar to that of the noise-normalized receiver. The performance of the self-normalized receiver for FFH/MFSK systems using convolutional coding and soft decision Viterbi decoding in a nonfading channel was previously examined. Using the union Chernoff bounds to calculate performance and neglecting the effects of thermal noise, Cheun and Stark showed that for  $M=8$ , the self-normalized receiver's performance was almost identical to that of the conventional receiver with perfect side information [Ref. 10].

This thesis calculates the performance of the FFH/BFSK self-normalized receiver in a different manner. First, the channel is assumed to be a Rician fading channel to provide a more general result. Secondly, the effects of thermal noise on the combining losses in a diversity system are considered. Thermal noise is often neglected in performance analysis to simplify computations. However, thermal noise is a factor when determining the optimum system parameters such as level of diversity and weighting strategy. It is shown that the conventional receiver with perfect side information is not an ideal system when the signal to thermal noise ratio is low relative to the signal to jammer power ratio. Also, the change in SNR is shown to change the level of diversity in combination with convolutional coding and soft decision Viterbi decoding required for optimal performance of the self-normalized receiver under conditions of partial-band jamming. This thesis examines the effects of varying the diversity of the system and of varying the constraint length of the code to gain insight into achieving optimal performance. Performance with convolutional coding is calculated numerically without use of the union Chernoff bound to obtain more accurate results.

## II. OVERVIEW OF SYSTEMS

### A. SPREAD SPECTRUM OVERVIEW

Spread spectrum communications systems have two fundamental characteristics. First, the bandwidth required to transmit the spread spectrum signal is much larger than the information bit rate. Secondly, the pseudo-randomness of the signal makes it difficult to intercept by anyone other than the intended receiver. [Ref. 11]

In addition to using a greater bandwidth, spread spectrum communications have the disadvantage of requiring more complex receivers and transmitters. In many applications, particularly in the military, the advantages of spread spectrum communications outweigh the disadvantages. Spread spectrum techniques can decrease the negative effects of narrowband interference which may be due to a hostile jammer or simply due to other users on the channel. Spread spectrum techniques such as direct sequence spread spectrum (DS/SS) hide the signal in background noise by spreading the signal bandwidth with coding [Ref.12]. The resulting signal has a low average power and is difficult to intercept or detect by anyone but the intended receiver. Such a signal is a low probability of intercept (LPI) signal [Ref. 6]. Although more easily detected than DS/SS, frequency-hopped spread spectrum systems (FH/SS) are also low probability of intercept since the signal is transmitted over a randomly changing frequency pattern known only by the transmitter and receiver. FH/SS is discussed in greater detail in the sections that follow. [Ref. 6]

### B. FREQUENCY-HOPPED SPREAD SPECTRUM

In frequency-hopped spread spectrum, the available channel bandwidth is divided into a large number of equally sized frequency slots. The transmitted symbol occupies one

of the available frequency slots. The choice of the slot is made by using a pseudo-noise (PN) sequence which is used to change the carrier frequency,  $f_c$ , periodically. Only the transmitter and receiver have the correct PN sequence and, thus, the choice of frequency slots appears random to an outside observer.

A frequency-hopping system can be characterized as either fast frequency-hopped (FFH) or slow frequency-hopped (SFH). The characterization of the system as fast or slow is dependent upon the relationship between the symbol rate and the hopping rate. If the symbol rate is greater than the hopping rate then the system is described as SFH. If the hopping rate is greater than or equal to the symbol rate then the system is FFH. Denoting  $T_h$  as the time between hops and denoting  $T_s$  as the symbol time, we have for fast frequency-hopping  $T_s = LT_h$  where  $L$  is an integer greater than or equal to 1. In this thesis, FFH is assumed.

FFH can be viewed as a combination of frequency and time diversity with the level of diversity equal to  $L$  [Ref. 13]. The use of diversity is an effective method to combat the effects of partial-band jamming and channel fading [Ref. 11].

### **C. FAST FREQUENCY-HOPPED BINARY FREQUENCY-SHIFT KEYING (FFH/BFSK)**

The modulation scheme used in FFH systems is generally noncoherent BFSK or M-ary Frequency Shift Keying (MFSK). Coherent detection currently is not practical since for FFH systems it is difficult for the receiver to maintain phase coherence between hops. In this section, the components of a conventional FFH/BFSK system are examined: the transmitter, receiver, and channel. Explanation of the self-normalized receiver and the conventional receiver with perfect side information require only a modification of the conventional FFH/BFSK receiver with no side information. The transmitter and channel

are the same for all three systems. Figure 2.1 shows the model of a conventional FFH/BFSK

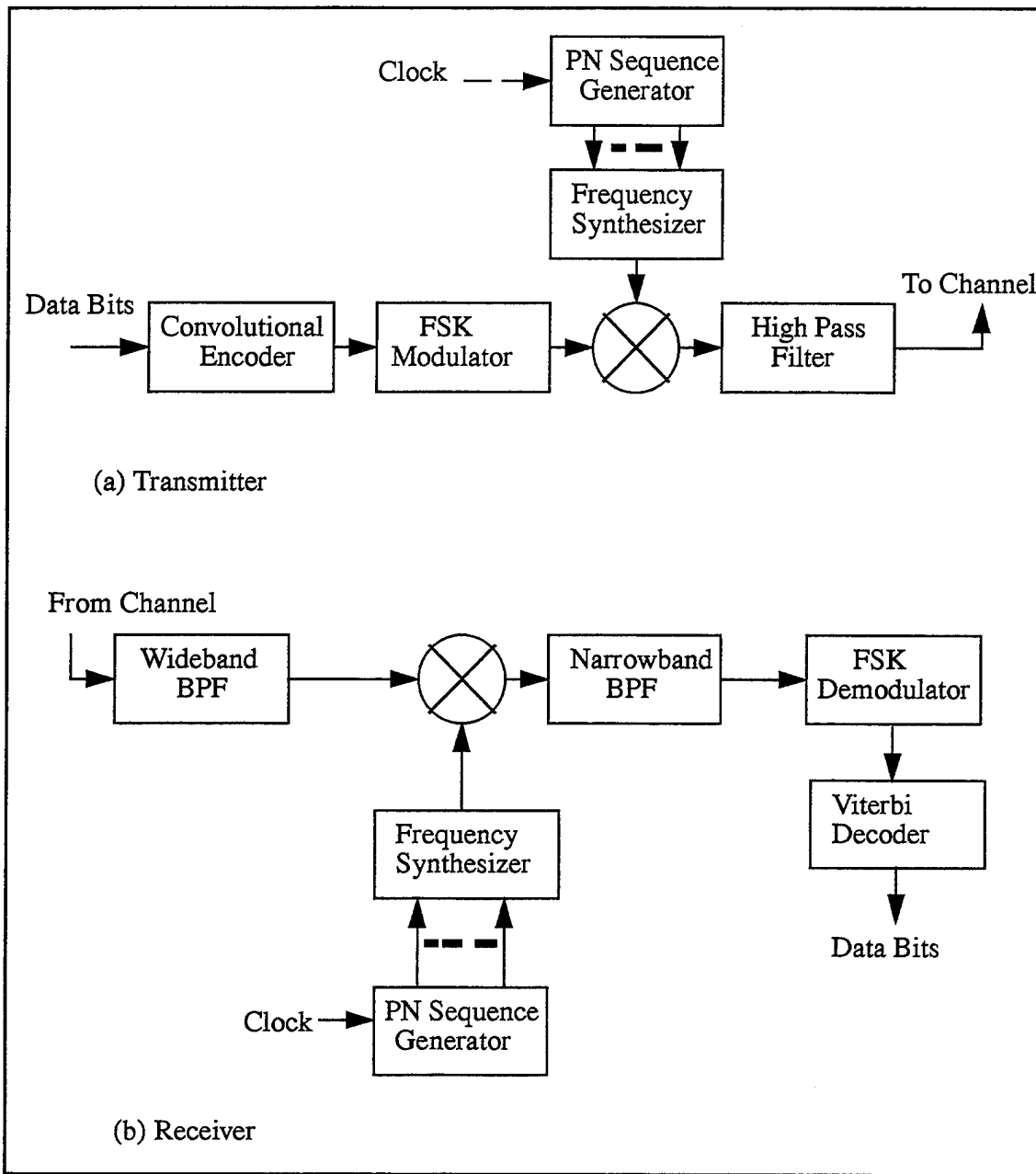


Figure 2.1: FFH/BFSK System Model with Convolutional Coding

spread spectrum transmitter and receiver with forward error correction coding. At the transmitter, the information sequence is encoded into a binary sequence of bits. The data

bits are then encoded using a convolutional encoder. The encoder takes  $k$  input bits and outputs  $n$  coded bits or symbols. The details of convolutional coding and its effects on the system are explained in a later section. The symbols are next modulated using BFSK signalling. The BFSK signal is of the form:

$$x(t) = \begin{cases} \sqrt{2}A_c[\cos 2\pi(f_c + \Delta f/2)t + \theta_0] & \text{symbol} = 0 \\ \sqrt{2}A_c[\cos 2\pi(f_c - \Delta f/2)t + \theta_1] & \text{symbol} = 1 \end{cases} \quad (2.1)$$

where  $\theta_n$   $n=1, 2$  is the unknown phase and  $\Delta f$  Hz is the minimum frequency separation required for orthogonal signalling. For a system of diversity of  $L$ ,  $\Delta f$  is equal to an integer multiple of the hop rate  $R_h = LR_s$  where  $R_s$  is defined as the symbol rate. Next the BFSK signal is spread by mixing it with the output of the frequency synthesizer  $y(t)$ :

$$y(t) = 2 \cos[2\pi(f_1 + (i-1)\Delta f_{fh})t + \theta_{s_i}], \quad i \in 1, \dots, N \quad (2.2)$$

where  $f_1$  is the lowest carrier frequency,  $\Delta f_{fh}$  is the frequency separation between adjacent bins,  $N$  is the total number of frequency bins, and  $\theta_{s_i}$  is the unknown phase of the synthesizer. The frequency bin location of each hop is determined by a PN sequence generator which drives the frequency synthesizer. The sequence generator is driven by a clock pulse which changes the generator output and, thus, the frequency bin once every  $T_h$  seconds. The hopping pattern appears random to anyone but the intended receiver.

The mixer produces a sum and difference frequency. With no overlap of the sum and difference frequency bands, the difference frequency can be removed by high pass filtering and the resulting transmitted signal is

$$s(t) = \sqrt{2}A_c \cos[2\pi(f_c + f_1 + (i-1)\Delta f_{fh} \pm \Delta f/2)t + \theta], \quad i \in 1, \dots, N \quad (2.3)$$

where  $\theta$  is the combined phase uncertainty and  $\pm$  represents the data (1/0). If  $\Delta f_{fh}$  is chosen as an integer multiple of  $2R_h$ , then all signals,  $s(t)$ , can be shown to be orthogonal over one hop duration,  $T_h$ . In this thesis, minimum frequency separation required for

orthogonal signalling is assumed and  $\Delta f = 1/T_h$  and  $\Delta f_{fh} = 2/T_h$ .

For the FFH/BFSK receiver shown in Fig. 2.1, it is assumed that the receiver's PN sequence generator is identical to the transmitter's. The phase of the receiver's PN sequence must also be aligned with that of the transmitter. Code acquisition is the determination of the initial code phase while code tracking involves maintaining code synchronization after acquisition [Ref. 6]. In this thesis, it is assumed that the receiver performs perfect code acquisition and code tracking and that the receiver has perfect bit synchronization. The multiplication of the received signal,  $r(t)$ , by the output of the frequency synthesizer is defined as despreading or dehoppping. After despreading, the input to the BFSK demodulator is composed of a sum and difference term. By filtering out the high frequency components, the standard BFSK signal given by (2.1) is recovered. A standard BFSK demodulator with diversity is shown in Fig. 2.2. The receiver employs noncoherent detection of the  $L$  hops using quadratic detectors, with one detector tuned to  $f_c + \Delta f/2$  corresponding to a bit 1 and the other tuned to  $f_c - \Delta f/2$  corresponding to a bit 0. The  $L$  samples  $\{x_{1k}, x_{2k}; k=1, 2, \dots, L\}$  in each channel are then summed to form the decision variables  $X_1$  and  $X_2$ . The difference  $Z = X_1 - X_2$  is then quantized and input into the Viterbi decoder.

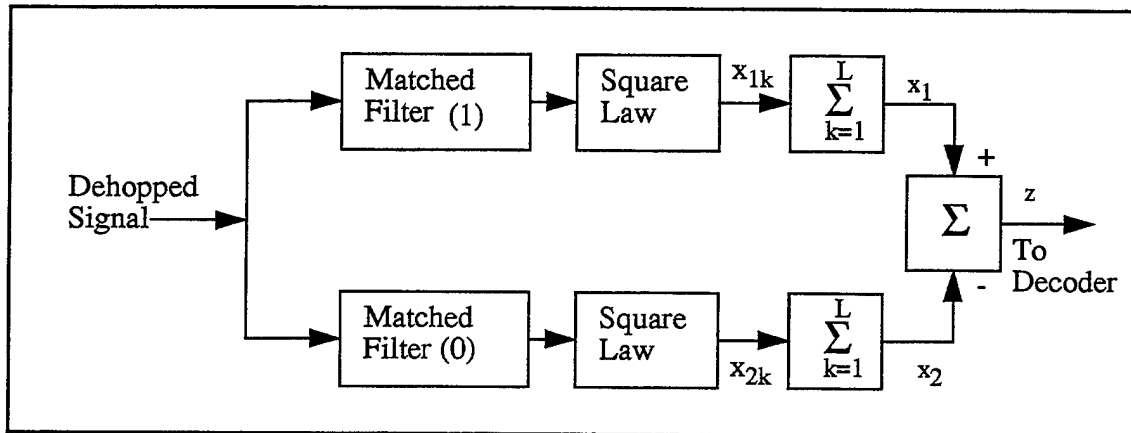


Figure 2.2: Standard BFSK Demodulator

The level of quantization of  $Z$  determines the type of decoding performed by the Viterbi decoder. As will be further explained below, two level quantization corresponds to hard decision decoding while infinite quantization corresponds to soft decision decoding.

#### **D. SOURCES OF PERFORMANCE DEGRADATION**

The FFH/BFSK system as described so far performs without error. A bit transmitted will be correctly received. Three sources of performance degradation are considered in this thesis: thermal noise, partial-band jamming, and multipath fading.

##### **1. Thermal Noise**

The thermal noise,  $n(t)$  in the system is modeled as zero-mean additive white Gaussian noise (AWGN) with two-sided power spectral density  $N_o/2$ . The noise power per hop at the receiver output due to AWGN is then

$$\sigma_k^2 = N_o B \quad (2.4)$$

where  $B=R_h$  is the minimum noise equivalent bandwidth of each branch of the FSK demodulator. It is assumed that the AWGN interference is not affected by fading.

##### **2. Partial-Band Interference**

The interference considered is partial-band noise interference which is assumed to be the result of a smart jammer. The smart jammer has complete knowledge of the spread-spectrum system design except for the exact frequency-hopping sequence. The jammer is then capable of transmitting the optimum or worst case partial-band jamming signal [Ref. 6]. The frequency-hopping signal will pseudo-randomly hop in and out of the jammed bandwidth and can be seriously degraded when in the jamming band.

For barrage jamming, the total jamming power of  $J$  watts is uniformly distributed over the entire spread spectrum bandwidth of  $W=2NB$  Hz. The interference is modeled as bandlimited AWGN, and has a two-sided power spectral density (psd) of

$$\frac{N_I}{2} = \frac{J}{2W} \quad (2.5)$$

For partial-band jamming, a fraction of the spread bandwidth,  $\gamma W$ , is jammed. Assuming constant  $J$ , the two-sided psd of the noise is

$$\frac{N_I}{2} = \frac{J}{2\gamma W} = \frac{N_I}{2\gamma} \quad (2.6)$$

The interference is then assumed to be present in both branches of the BFSK demodulator for any reception of the dehopped signal with probability  $\gamma$  and not present with probability  $1-\gamma$ . It is assumed that an integral number of frequency hop bins are jammed, and the bounds on  $\gamma$  are

$$1 \geq \gamma \geq \frac{1}{N} \quad (2.7)$$

The combined psd of the thermal noise and the partial-band noise interference is

$$\frac{N_T}{2} = \frac{N_I}{2\gamma} + \frac{N_o}{2} \quad (2.8)$$

and the total noise power for a hop  $k$  of a symbol is

$$\sigma_k^2 = \left( N_o + \frac{N_I}{\gamma} \right) B \quad (2.9)$$

The use of frequency-hopping spread spectrum is helpful in mitigating the effects of hostile jamming. Frequency-hopping requires a barrage jammer to jam  $N$  times as much bandwidth as would be required if a conventional BFSK system were used. Since the jammer is assumed to be power limited, the jammer must spread its power over a larger frequency band to jam the same fraction of the bandwidth and as a result will be less effective.

### 3. Fading Multipath Channel

Multipath fading can have a significant effect on the signal-to-noise power ratio of a digital communications system. When the FFH/BFSK signal is sent through the channel,

multiple copies of the signal will be received due to scattering and reflections in the medium. The reflected components of the signal travel along different paths from the receiver to the transmitter resulting in a time and phase delay relative to line-of-sight (direct) components of the signal. Due to different phases, the component signals will add constructively and destructively resulting in amplitude variations of the received signal. The amplitude of the signal is described in statistical terms with random and time variant characteristics. [Ref. 11]

Several assumptions are made in this thesis regarding channel fading. First, it is assumed that the data signal bandwidth is much less than the coherence bandwidth of the channel, hence the channel is frequency-nonselctive. All frequencies within a hopping bin are affected statistically the same by the channel. Next, it is assumed that the channel is slowly fading. Hence, the time varying characteristics of the channel remain constant over the signal duration. Also, a slowly changing channel has a small Doppler spread. Finally, the channel is modeled as Rician, which implies that for a received, despread signal of amplitude  $\sqrt{2}a_k$  that  $a_k$  is modeled as a Rician random variable [Ref. 14], with a probability density function given by

$$f_{A_k}(a_k) = \frac{a_k}{\sigma^2} \cdot \exp\left(-\frac{a_k^2 + \alpha^2}{2\sigma^2}\right) I_0\left(\frac{a_k\alpha}{\sigma^2}\right) u(a_k) \quad (2.10)$$

where  $\alpha^2$  is the average power of the direct component of the signal,  $2\sigma^2$  is the average power of the diffuse component of the signal,  $u(\bullet)$  is the unit step function, and  $I_0(\bullet)$  is the modified Bessel function. The total power of a hop is then equal to  $\alpha^2 + 2\sigma^2$ . In this thesis,  $\alpha^2 + 2\sigma^2$  is assumed constant for all hops. The direct-to-diffuse power ratio is defined

$$\eta = \frac{\alpha^2}{2\sigma^2} \quad (2.11)$$

If  $\alpha^2 = 0$  then  $\eta = 0$  and there is no direct component to the signal. In this case, the channel is a Rayleigh fading channel. If  $2\sigma^2 = 0$  this implies  $\eta \rightarrow \infty$  and there is no fading. [Ref. 5]

Channel fading can have a severe effect on system performance. For a conventional BFSK system in a Rician fading channel, the error rates decrease only inversely with SNR as opposed to an exponential decrease in a nonfading channel. The use of diversity is known to mitigate the effects of fading. Since FFH hopping is a form of frequency and time diversity it is not surprising that research has shown that the use of FFH/BFSK will improve performance over a conventional BFSK system without diversity. [Ref. 11]

#### **E. FORWARD ERROR CORRECTION**

Even with the use of spread spectrum communications, a worst case partial-band jammer can significantly degrade system performance [Ref. 6]. Thus, some form of forward error correction coding is required for reliable communications. The FFH/BFSK system shown in Fig. 2.1 contains error correction to combat the effects of interference and of multipath fading. Convolutional coding with Viterbi decoding has become one of the most common forward error correction techniques and is assumed for this system.

A convolutional code is created by inputting the information sequence into a linear finite state shift register. The encoder produces  $n$  coded bits from  $k$  data bits and  $k(v-1)$  of the preceding data bits where the parameter  $v$ , the constraint length, is one plus the number of stages in the shift register. The rate of the code is defined as:

$$r = k/n. \quad (2.12)$$

In this thesis consideration is limited to  $k=1$  and  $n=2$  or  $3$ . The output of the encoder is the result of the incoming data bit and the  $v-1$  previous inputs. The complexity of the decoding operation for a convolutional code increases exponentially with increasing constraint length and becomes impractical for large  $v$ . This analysis looks at decoders with constraint

lengths up to nine which is the current limit for most integrated-circuit Viterbi decoders.[Ref. 6]

The encoded data sequence can be viewed as the mapping of a continuous sequence of information bits onto a continuous sequence of encoder output bits which are then transmitted through the channel. The sequence is decoded using the Viterbi decoding algorithm which is a maximum likelihood decoder providing the minimum probability of bit error. The convolutional code can be defined using a trellis structure [Ref. 15]. Each codeword represents a semi-infinite path through the trellis. The Viterbi algorithm compares the received codeword to each of the possible paths. A distance measure or branch metric is generated for each path. The paths with the largest distance from the received sequence are dynamically eliminated and the path with the smallest distance from the received sequence, or equivalently the largest branch metric, is retained. The path then becomes the corrected codeword and, assuming the correct path is chosen, any errors in the received codeword are removed.

There are two types of decisions, hard or soft, which can be made by the decoder. In either case, the complexity of implementation is similar. Hard decision decoding occurs when the output of the BFSK demodulator, the code-bit metric is quantized with only two levels, e.g. 1 or 0. For soft decision decoding, the distance metric is quantized to more than two levels prior to entrance into the decoder. The use of soft decision decoding provides the decoder with information regarding the reliability of its decoding decision. Such information can be viewed as a type of side information. Infinite quantization levels give the best performance, but implementation is impractical. It has been shown, however, by Clark and Cain [Ref. 15] that there is only a slight difference between eight level quantization and infinite quantization. In this thesis, regarding soft decision decoding, infinite quantization is assumed.

The measure used to determine the decoding reliability for Viterbi decoding is the probability that the correct path through the trellis is discarded as the decoder proceeds through the trellis. Since convolutional codes are linear, the decoding error probability of

all possible transmitted sequences are equal and the all zero code-word can be assumed to be sent for ease of analysis. The union bound on the probability of bit error using convolutional coding is defined as [Ref. 15]:

$$P_b < \frac{1}{k} \sum_{d=d_{\text{free}}}^{\infty} w_d P_2(d). \quad (2.13)$$

Here,  $P_2(d)$  is the error probability between two codewords which differ in  $d$  symbols. The total information weight,  $w_d$ , is the total number of bit errors associated with all paths which differ in  $d$  symbols from the all zero symbol path. The lower bound on  $d$ ,  $d_{\text{free}}$ , is equal to the minimum Hamming distance between any two distinct code sequences. The constant,  $k$ , is the number of inputs at the encoder which in this thesis is assumed to be equal to one. Since increasing the constraint length of a code is not always practical, a method to increase the free distance of a code is to repeat each symbol  $L$  times [Ref. 11]. The result is a convolutional code with a minimum free distance of  $Ld_{\text{free}}$ . For error rate performance with repetitions (diversity) (2.13) becomes

$$P_b < \frac{1}{k} \sum_{d=d_{\text{free}}}^{\infty} w_d P_2(Ld). \quad (2.14)$$

For hard decision decoding, the probability of selecting the incorrect path if  $d$  is odd is,

$$P_2(d) = \sum_{k=\frac{d+1}{2}}^d \binom{d}{k} p^k (1-p)^{d-k} \quad (2.15)$$

and if  $d$  is even is

$$P_2(d) = \sum_{k=\frac{d}{2}+1}^d \binom{d}{k} p^k (1-p)^{d-k} + \frac{1}{2} \binom{d}{d/2} p^{d/2} (1-p)^{d/2} \quad (2.16)$$

where  $p$  is the symbol error probability of the channel [Ref. 11].

For soft decision decoding, Clark and Cain [Ref. 15] have shown that, assuming noncoherent detection with square law detectors (as used in the self-normalizing receiver and conventional BFSK receivers), the probability of error in comparing a weight zero path with a weight  $d$  path is equivalent to the probability of error in noncoherent combining of  $d$  transmissions. Thus the use of convolutional coding is analogous to using diversity with constant energy per hop. This fact will become the basis for the analysis of the coded performance of the conventional receiver with perfect side information and the self-normalizing receiver.

Convolutional coding performs best when the channel errors are independent. The worst case partial band jammer will produce burst errors for frequency hopped systems. Thus a block interleaver is assumed between the encoder and the modulator and a de-interleaver is placed between the demodulator and the decoder. [Ref. 6]

## F. ENERGY AND BANDWIDTH CONSIDERATIONS

To make a fair comparison of different systems, assumptions regarding bit energy and bandwidth must be clearly defined. An FFH/BFSK system with diversity can be classified as constant energy per bit,  $E_b$ , with varying diversity or as constant energy per hop,  $E_h$  with varying diversity. In a constant energy per bit system each coded bit or symbol, represented by a signal of duration  $T_s$  seconds, is broken down into  $L$  independent transmissions (hops) represented by signals of duration  $T_h = T_s/L$  seconds. Defining  $S$  as the signal power and  $E_s$  as the energy of a signal representing a symbol or coded bit, we have the relationships

$$E_s = rE_b = LE_h = LST_h. \quad (2.17)$$

For a constant energy per bit system  $T_h$  decreases as  $L$  increases. Also, the bandwidth of a frequency bin,  $B = 2/T_h$ , increases by a factor of  $L$  over a no diversity system. The advantage of a constant energy per bit system is that the data rate remains constant as

diversity increases. If the number of frequency bins,  $N$ , is held constant the spread bandwidth,  $W=2NR_h$  is expanded by a factor of  $L$ . Since increasing  $W$  requires the jammer to spread its power over a wider bandwidth, the use of diversity can be considered as a possible method to mitigate the effects of the jammer.

For a constant energy per hop system the relationship of (2.17) remains where now  $T_h$  and  $E_h$  are constant. For such a system the received symbol energy  $E_s = LE_h$  increases with diversity. Increasing diversity then increases the symbol energy to total interference psd,  $E_s/N_T$ . In theory,  $L$  can be increased to a high enough level to combat the effects of any jammer interference. The disadvantage of such a system is that the data rate,  $R_b$ , decreases with increasing diversity.

It is assumed in this thesis that the data or information rate,  $R_b$ , is unaffected by coding. The use of coding, thus, requires an increase in the hopping rate and is assumed in this thesis to expand the bandwidth of a frequency hopping bin by the factor of  $1/r$  over uncoded systems. Unless otherwise stated, constant energy per bit systems will be analyzed in this thesis. For comparison purposes an example of the performance of constant energy per hop systems is shown in Ch. VI.

## **G. THE SELF-NORMALIZED RECEIVER**

The disadvantage of the conventional FFH/BFSK receiver with diversity in the presence of partial band jamming is that all hops are weighted equally whether jammed or unjammed. Miller, French and Lee shown that there is no diversity improvement for a linear combining receiver against partial-band noise. In the absence of fading, performance actually degrades as diversity increases due to noncoherent combining losses. [Ref. 1]

The self-normalized receiver is a nonlinear combining receiver where the detected hops are used to calculate the normalization factors. The structure of the self-normalized receiver, shown in Fig. 2.3, is a slight modification of the structure of the conventional

FFH/BFSK receiver. It is seen that in self-normalizing combining the outputs of the two quadratic detectors are summed after each hop and used to normalize the output of each detector before the L hop receptions are combined. The normalized random variables  $Z_{1k}$  and  $Z_{2k}$  are given by:

$$Z_{ik} = \frac{X_{ik}}{X_{1k} + X_{2k}}, \quad i=1,2. \quad (2.18)$$

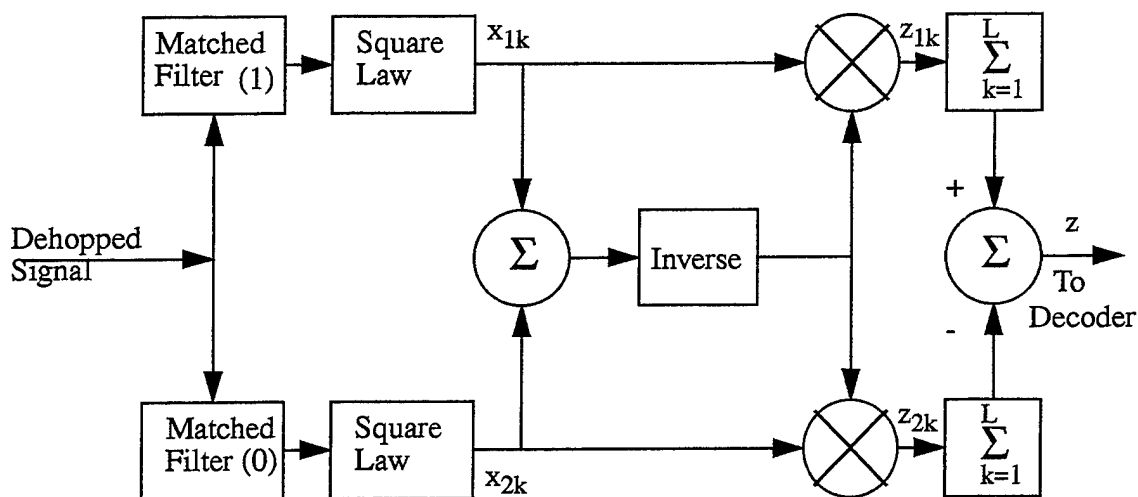


Figure 2.3: Self-normalization Combining FFH/BFSK Receiver

As a result of the normalization, the output of each detector will be smaller when the hop contains a large amount of interference. Therefore, hops without interference or jamming will have a greater influence on the output,  $z$ , than hops which contain interference. It can be seen that self-normalizing is a practical method to weight hops with performance which will be similar to that of a conventional receiver with perfect side information. The performance analysis of a receiver with perfect side information is detailed in Chapter III. This performance can then be compared to the performance of the self-normalized receiver which is analyzed in Chapter IV.

### III. PERFORMANCE ANALYSIS FOR FFH/BFSK CONVENTIONAL RECEIVER WITH PERFECT SIDE INFORMATION AND CONVOLUTIONAL CODING

For analysis of a conventional receiver with perfect side information, we assume a jammer state estimator is added to the system of Fig. 2.1. The jammer state estimator outputs a 1 if the received hop is jammed and a 0 if the hop is not jammed. A soft decision Viterbi decoder can make use of this reliability information. The decoder drops those  $i$  jammed hops from the total of  $dL$  hops per codeword. A hard decision decoder is unable to use reliability information. If a hard decision decoder is used, the jammer state information is assumed to be used by the demodulator which drops the  $i$  jammed hops from the total of  $L$  hops per bit. These assumptions regarding soft and hard decision decoding for the conventional receiver with perfect side information allow a fair comparison with the self-normalized receiver.

#### A. PERFORMANCE WITHOUT FADING

The probability of bit error,  $P_b$ , for a BFSK/FFH conventional receiver with  $L$  fold diversity in the presence of partial-band jamming is

$$P_b = \sum_{i=0}^L \Pr(i \text{ hops jammed}) \times P_b(i) \quad (3.1)$$

$$= \sum_{i=0}^L \binom{L}{i} \gamma^i (1-\gamma)^{(L-i)} P_b(i) \quad (3.2)$$

where  $P_b(i)$  is defined as the conditional bit error probability given  $i$  hops are jammed [Ref. 1]. If  $i$  is less than  $L$ , the receiver with perfect side information disregards  $i$  jammed hops and uses the remaining  $L-i$  hops. If all  $L$  hops are jammed then the receiver must use all available hops. In this case side information offers no advantage. The probability of bit

error for a receiver with perfect side information given all  $L$  hops are jammed is equivalent to that of a conventional receiver with no side information and is given by [Ref. 11]

$$P_b(L) = \frac{1}{2} \exp \left[ \frac{-LE_h}{2 \left( N_o + \frac{N_I}{\gamma} \right)} \right] \sum_{n=0}^{L-1} c_n \left[ \frac{LE_h}{2 \left( N_o + \frac{N_I}{\gamma} \right)} \right]^n \quad (3.3)$$

$$= \frac{1}{2} \exp \left[ \frac{-E_b}{2 \left( N_o + \frac{N_I}{\gamma} \right)} \right] \sum_{n=0}^{L-1} c_n \left[ \frac{E_b}{2 \left( N_o + \frac{N_I}{\gamma} \right)} \right]^n \quad (3.4)$$

where

$$c_n = \frac{1}{n!} \sum_{m=0}^{L-1-n} \frac{1}{2^{L-1+m+n}} \binom{L-1+n+m}{m} . \quad (3.5)$$

If  $i$  hops are jammed where  $i$  is less than  $L$ , then the conditional probability of bit error,  $P_b(i)$ , given  $i$  hops jammed is obtained by replacing  $L$  in (3.3) and (3.5) with  $L-i$  to obtain [Ref. 13]:

$$P_b(i) = \frac{1}{2} \exp \left[ \frac{-(L-i)(E_b/L)}{2N_o} \right] \sum_{n=0}^{L-i-1} c_n(i) \left[ \frac{(L-i)(E_b/L)}{2N_o} \right]^n \quad (3.6)$$

where

$$c_n(i) = \frac{1}{n!} \sum_{m=0}^{L-i-1-n} \frac{1}{2^{L-i-1+m+n}} \binom{L-i-1+n+m}{m} . \quad (3.7)$$

The system performs as a receiver with diversity of order  $(L-i)$  in the presence of AWGN and no jamming. The total probability of bit error for a conventional receiver with perfect side information is obtained by combining (3.2), (3.4) and (3.6) to obtain:

$$P_b = \gamma^L P_b(L) + \sum_{i=0}^{L-1} \binom{L-1}{i} \gamma^i (1-\gamma)^{(L-i-1)} P_b(i) . \quad (3.8)$$

We use (2.14) to find the probability of bit error for the conventional receiver with perfect side information when convolutional coding with soft decision decoding is added. Each demodulator output corresponding to a hop represents one code symbol. The error probability between two codewords which differ in  $dL$  symbols is

$$P_2(dL) = \gamma^{dL} P_s(dL) + \sum_{i=0}^{dL-1} \binom{dL-1}{i} \gamma^i (1-\gamma)^{(dL-i-1)} P_s(i) \quad (3.9)$$

where  $P_s(i)$  is the error probability given  $i$  coded hops are jammed. If  $E_h$  is defined as the energy in a signal corresponding to an uncoded hop then  $rE_h$  is the energy corresponding to the energy of a coded hop. The probability of error given  $dL$  hops are jammed is found from (3.3) and (3.5) by replacing  $L$  with  $dL$  and  $E_h$  with  $rE_h$ . Again noting that  $E_b = LE_h$ , we obtain

$$P_s(dL) = \frac{1}{2} \exp \left[ \frac{-drE_b}{2 \left( N_o + \frac{N_I}{\gamma} \right)} \right] \sum_{n=0}^{dL-1} c_n \left[ \frac{drE_b}{2 \left( N_o + \frac{N_I}{\gamma} \right)} \right]^n \quad (3.10)$$

where

$$c_n = \frac{1}{n!} \sum_{m=0}^{dL-1-n} \frac{1}{2^{dL-1+m+n}} \binom{dL-1+n+m}{m} \quad (3.11)$$

Similarly (3.6) and (3.7) become

$$P_s(i) = \frac{1}{2} \exp \left[ \frac{-(dL-i)(rE_b/L)}{2N_o} \right] \sum_{n=0}^{dL-i-1} c_n(i) \left[ \frac{(dL-i)(rE_b/L)}{2N_o} \right]^n \quad (3.12)$$

where

$$c_n(i) = \frac{1}{n!} \sum_{m=0}^{dL-i-1-n} \frac{1}{2^{dL-i-1+m+n}} \binom{dL-i-1+n+m}{m} \quad (3.13)$$

In these equations it is assumed that the uncoded L fold diversity system is a constant energy per bit system where  $E_h = \frac{E_b}{L}$ . As diversity, L, increases then the signal energy corresponding to a hop,  $E_h$ , decreases. The use of convolutional coding gives an equivalent diversity of d where the energy of a hop is now constant and the coded bit energy effectively increases with d.

## B. PERFORMANCE IN FADING CHANNELS

The probability of bit error for a conventional FFH/BFSK receiver in a Rician fading channel was found by Lindsey [Ref. 16]. Our evaluation of the performance of the receiver with perfect side information in a fading channel begins with the equation for the conventional receiver in a nonfading channel given L hops are jammed, (3.4). We substitute  $a_c^2 T_b$  for  $E_b$ , where  $a_c^2$  is the average power of a received bit. Also by replacing the total noise psd,  $N_o + \frac{N_I}{\gamma}$ , with  $\sigma_k^2 T_b$ , we obtain the following equivalent equation for the probability of bit error for a conventional receiver with L fold diversity in a nonfading channel.

$$P_b(L) = \frac{1}{2} \exp\left(\frac{-a_c^2}{2\sigma_k^2}\right) \sum_{n=0}^{L-1} c_n \left(\frac{a_c^2}{2\sigma_k^2}\right)^n \quad (3.14)$$

In a nonfading channel, the amplitude of each hop is  $\sqrt{2}a_{ck}$  and is assumed constant for every hop. Therefore, in a nonfading channel the total power in a bit is related to the total power in the L received hops by

$$a_c^2 = \sum_{k=1}^L a_{ck}^2 = L a_{ck}^2 \quad (3.15)$$

In a Rician fading channel the amplitude of each hop varies and  $a_{ck}$  is modeled as a Rician random variable with a probability distribution function (pdf) given by (2.10). If a new random variable  $\Sigma$  is defined as

$$\Sigma = \sum_{k=1}^L a_{ck}^2 \quad (3.16)$$

then (3.14) becomes a conditional bit error probability given  $\Sigma$ :

$$P_b(L|\Sigma) = \frac{1}{2} \exp\left(\frac{-\Sigma}{2\sigma^2}\right) \sum_{n=0}^{L-1} c_n \left(\frac{\Sigma}{2\sigma^2}\right)^n. \quad (3.17)$$

We now define an auxiliary random variable  $b_k = a_{ck}^2$  which is a non-central Chi-squared random variable with two degrees of freedom and with the probability density function given by [Ref. 14]:

$$f_B(b_k) = \frac{1}{2\sigma^2} \exp\left(-\frac{1}{2\sigma^2}(b_k + \alpha^2)\right) I_0\left(\frac{\alpha\sqrt{b_k}}{\sigma^2}\right) \quad (3.18)$$

where

$$\Sigma = \sum_{k=1}^L b_k. \quad (3.19)$$

Given the assumption, as discussed in Ch. 2, that each hop fades independently, then the  $b_k$ 's are independent random variables and, therefore,

$$f_{\Sigma}(\Sigma) = f_B(b_k)^{\otimes L} \Leftrightarrow F_{\Sigma}(s) = F_B(s)^L \quad (3.20)$$

where  $\otimes L$  implies  $L-1$  convolutions and  $F_B(s)$  is the Laplace transform of  $f_B(b_k)$ . By using the definition of the Laplace transform,

$$F_B(s) = \int_0^{\infty} f_B(b_k) \exp(-sb_k) db_k \quad (3.21)$$

we obtain

$$F_B(s) = \frac{1}{2\sigma^2} \left( \frac{1}{s + 1/(2\sigma^2)} \right) \exp \left[ \frac{-\alpha^2}{2\sigma^2} \left( \frac{s}{s + 1/(2\sigma^2)} \right) \right]. \quad (3.22)$$

We raise  $F_B(s)$  to the  $L^{\text{th}}$  power and then use the shifting property of the Laplace transform to find the inverse Laplace transform. This yields

$$f_\Sigma(\Sigma) = \frac{\Sigma^{(L-1)/2}}{2\sigma^2(L\alpha^2)^{(L-1)/2}} \exp \left( -\frac{(\Sigma + L\alpha^2)}{2\sigma^2} \right) I_{L-1} \left( \frac{\alpha\sqrt{L\Sigma}}{\sigma^2} \right) \quad (3.23)$$

where  $I_{L-1}(\bullet)$  is the modified Bessel function of the first kind and order  $L-1$  [Ref. 17, 18].

Now the probability of bit error for an  $L$  fold diversity system in a Rician fading channel can be obtained by integrating the conditional probability of (3.17) over  $\Sigma$ ,

$$P_b(L) = \int_0^\infty P_b(L|\Sigma) f_\Sigma(\Sigma) d\Sigma \quad (3.24)$$

resulting in

$$P_b(L) = \frac{1}{4\sigma^2(L\alpha^2)^{(L-1)/2}} \exp \left( -\frac{L\alpha^2}{2\sigma^2} \right) \sum_{n=0}^{L-1} c_n 1/(2\sigma_k^2)^n \Gamma \quad (3.25)$$

where

$$\Gamma = \int_0^\infty \Sigma^{n+(L-1)/2} \exp \left[ -\frac{\Sigma}{2} \left( \frac{1}{\sigma^2} + \frac{1}{\sigma_k^2} \right) \right] I_{L-1} \left( \frac{\alpha\sqrt{L\Sigma}}{\sigma^2} \right) d\Sigma_k. \quad (3.26)$$

The integral in  $\Gamma$  can be evaluated using [Ref. 19, p. 741] to obtain

$$\Gamma = n! \left( \frac{\sqrt{L}\alpha}{2\sigma^2} \right)^{L-1} \left( \frac{2\sigma^2\sigma_k^2}{\sigma_k^2 + \sigma^2} \right)^{m+L} \exp \left( \frac{2L\alpha^2}{2\sigma^2(2+\xi)} \right) \mathcal{L}_m^{L-1} \left( \frac{-2L\eta}{2+\xi} \right) \quad (3.27)$$

where  $\rho_k = \alpha^2/\sigma_k^2$  is defined as the signal-to-noise ratio of the direct component of hop

k of a bit,  $\xi_k = 2\sigma^2/\sigma_k^2$  is defined as the signal-to-noise ratio of the diffuse component of hop k of a bit, and  $L_m^{L-1}$  is the Laguerre polynomial. Combining (3.25) and (3.27), using the definition of the Laguerre polynomial [Ref. 19, p. 1061], and simplifying, we obtain a closed form solution for the probability of bit error for an L fold diversity system in a Rician fading channel:

$$P_b(L) = \frac{1}{2} \left( \frac{2}{2 + \xi_k} \right)^L \exp\left(-\frac{L\rho}{2 + \xi_k}\right) \sum_{n=0}^{L-1} c_n n! \left( \frac{\xi_k}{2 + \xi_k} \right)^n d_p \quad (3.28)$$

where

$$d_p = \sum_{p=0}^n \frac{1}{p!} \binom{n+L-1}{n-p} \left( \frac{2L\eta}{2 + \xi_k} \right)^p \quad (3.29)$$

and where  $\eta = \rho_k/\xi_k$  is defined as the ratio of the direct-to-diffuse signal power. Next the noise power with and without jamming is defined as:

$$\sigma_o^2 = N_o B \quad (3.30)$$

and

$$\sigma_j^2 = \left( \frac{N_I}{\gamma} + N_o \right) B \quad (3.31)$$

respectively.

The union bound on the probability of bit error for a FFH/BFSK conventional receiver with perfect side information with soft decision decoding in the presence of partial-band jamming and for a Rician fading channel is obtained by again using (2.14) and (3.9).  $P_s(dL)$  is obtained by replacing L with dL in (3.28) and (3.29) to obtain

$$P_s(dL) = \frac{1}{2} \left( \frac{2}{2 + \xi_j} \right)^{dL} \exp\left(-\frac{dL\rho_j}{2 + \xi_j}\right) \sum_{n=0}^{dL-1} c_n n! \left( \frac{\xi_j}{2 + \xi_j} \right)^n d_p \quad (3.32)$$

where

$$d_p = \sum_{p=0}^n \frac{1}{p!} \binom{n+dL-1}{n-p} \left( \frac{2dL\eta}{2+\xi_j} \right)^p. \quad (3.33)$$

Performing the same substitutions for the case of  $i$  hops jammed, we obtain

$$P_s(i) = \frac{1}{2} \left( \frac{2}{2+\xi_o} \right)^{dL-i} \exp\left(-\frac{(dL-i)p}{2+\xi_o}\right) \sum_{n=0}^{dL-i-1} c_n n! \left( \frac{\xi_o}{2+\xi_o} \right)^n d_p \quad (3.34)$$

where

$$d_p = \sum_{p=0}^n \frac{1}{p!} \binom{m+dL-i-1}{n-p} \left( \frac{2(dL-i)\eta}{2+\xi_o} \right)^p. \quad (3.35)$$

It can be seen that as  $\eta \rightarrow \infty$  the solution for probability of bit error for a Rician fading channel matches the solution for a nonfading channel.

## IV. PERFORMANCE ANALYSIS FOR FFH/BFSK SELF-NORMALIZED RECEIVER WITH CONVOLUTIONAL CODING

### A. ANALYSIS

For the analysis of the self-normalized receiver we desire to find the probability of bit error versus the  $E_b/N_I$  given a Rician fading channel. A model equivalent of a FFH/BFSK self-normalized receiver employing convolutional coding with soft decision Viterbi decoding is shown in Fig. 4.1. Performance analysis of the self-normalized receiver without coding was performed previously for the nonfading [Ref. 4] and fading [Ref. 5] cases. In these papers, the statistics of the sampled outputs  $x_{1n}$  and  $x_{2n}$  of the quadratic detector and of the normalized samples  $z_{1n}$  and  $z_{2n}$ , for any hop  $n$ , before diversity combining were derived. The bit error probability with convolutional coding is determined by using these previous derivations as a basis.

It is assumed without loss of generality that the signal is present in the branch 1 of the demodulator. The conditional probability density function of the quadratic detector output of branch 1 has been shown to be [Ref. 14]

$$f_{X_{1n}}(x_{1n}|a_n) = \frac{1}{2\sigma_n^2} \exp\left(-\frac{x_{1n} + 2a_n^2}{2\sigma_n^2}\right) I_0\left(\frac{a_n\sqrt{2x_{1n}}}{\sigma_n^2}\right) u(x_{1n}) \quad (4.1)$$

where  $u(\bullet)$  is the unit step function,  $a_n$  is the Rician random variable of (2.10) representing the fading of hop  $n$  and  $\sigma_n^2$  is defined as the noise power in a hop corresponding to a signal amplitude of  $\sqrt{2}a_n$ . The probability density function of the random variable  $X_{1n}$  is given by the integration

$$f_{X_{1n}}(x_{1n}) = \int_0^{\infty} f_{X_{1n}}(x_{1n}|a_n) f_{a_n}(a_n) da_n \quad (4.2)$$

which has been found to be [Ref. 5]

$$f_{X_{1n}}(x_{1n}) = \frac{1}{2(\sigma_n^2 + \sigma^2)} \exp\left[-\frac{1}{2}\left(\frac{x_{1n} + 2\alpha^2}{\sigma_n^2 + 2\sigma^2}\right)^2\right] I_0\left(\frac{\alpha\sqrt{2x_{1n}}}{\sigma_n^2 + 2\sigma^2}\right) u(x_{1n}). \quad (4.3)$$

The pdf of the random variable  $X_{2n}$ , which corresponds to the output of branch 2 of the demodulator is found by, replacing  $x_{1n}$  with  $x_{2n}$  and letting  $\alpha^2 = 2\sigma^2 = 0$  with the result

$$f_{X_{2n}}(x_{2n}) = \frac{1}{2\sigma^2} \exp\left[-\frac{x_{2n}}{2\sigma^2}\right] u(x_{2n}). \quad (4.4)$$

The normalized random variable  $Z_{1n}$ ,  $i=1,2$  is given by (2.18). Defining  $v_n = x_{1n} + x_{2n}$  and using the Jacobian of the transformation  $J = v_n^{-1}$ , we obtain the pdf of  $Z_{1n}$  as

$$f_{Z_{1n}}(z_{1n}) = \int_0^{\infty} v_n f_{x_{1n}x_{2n}}[v_n z_{1n}, v_n(1-z_{1n})] dv_n \quad (4.5)$$

$X_{1n}$  and  $X_{2n}$  are independent random variables and, therefore, the joint probability density function is:

$$f_{X_{1n}, X_{2n}}(x_{1n}, x_{2n}) = f_{X_{1n}}(x_{1n}) \cdot f_{X_{2n}}(x_{2n}). \quad (4.6)$$

Using these relationships, Robertson and Ha found the solution to (4.5) be [Ref. 5]

$$f_{Z_{1n}}(z_{1n}) = \frac{\rho_n z_{1n} + (1 + \xi_n)[1 + \xi_n(1 - z_{1n})]}{[1 + \xi_n(1 - z_{1n})]^3} \quad (4.7)$$

$$\cdot \exp\left[\frac{-\rho_n(1 - z_{1n})}{1 + \xi_n(1 - z_{1n})}\right] \quad (0 \leq z_{1n} \leq 1)$$

where  $\xi_n$  and  $\rho_n$  are the signal-to-noise ratios of the diffuse and direct components, respectively, of a hop  $n$  of a bit as defined in Chapter III.

For the specific case of a nonfading channel  $\xi_n \rightarrow 0$  with the result from Miller, Lee and Kadrichu [Ref. 4]:

$$f_{Z_{1n}}(z_{1n}) = \exp(\rho_n + \rho_n z_{1n})[\rho_n z_{1n} + 1] \quad (0 \leq z_{1n} \leq 1). \quad (4.8)$$

When  $\rho_n \rightarrow 0$  we have a Rayleigh faded channel with the result:

$$f_{Z_{1n}}(z_{1n}) = \frac{(1 + \xi_n)}{[1 + \xi_n(1 - z_{1n})]^2} \quad (0 \leq z_{1n} \leq 1). \quad (4.9)$$

## B. PROBABILITY OF BIT ERROR

We determine the union bound on the bit error probability of the self-normalized receiver with convolutional coding and soft decision Viterbi decoding and diversity beginning with (2.14). We note that the Viterbi decoder is a maximum likelihood decoder. Also,  $P_2(dL)$  is the likelihood that the all zero path through the trellis is eliminated by a path of weight  $dL$ . Thus,  $P_2(dL)$  can be found by analyzing the equivalent system model shown in Fig. 4.1.

Now, the total number of hops is equal to  $dL$  and therefore,

$$P_2(dL) = \sum_{i=0}^{dL} \Pr(i \text{ hops jammed}) \times P_2(dL|i) \quad (4.10)$$

$$= \sum_{i=0}^{dL} \binom{dL}{i} \gamma^i (1 - \gamma)^{(dL-i)} P_2(dL|i) \quad (4.11)$$

where  $P_2(dL|i)$  is the conditional probability that the all zero path is eliminated by a path of weight  $dL$  given  $i$  hops are jammed. Now

$$P_2(dL|i) = \Pr(Z_c < 0|i) \quad (4.12)$$

$$= \Pr\left(\sum_{j=1}^d \Pr(Z_{1j} - Z_{2j}) < 0 | i\right) \quad (4.13)$$

$$= \Pr\left(\sum_{j=1}^d \sum_{n=1}^L \Pr(Z_{1nj} - Z_{2nj}) < 0 | i\right). \quad (4.14)$$

Now from (2.18) it can be seen that  $Z_{1nj} + Z_{2nj} = 1$ ; therefore  $Z_{2nj} = 1 - Z_{1nj}$ . Substitution for  $z_{2nj}$  in (4.14) and rearrangement of terms results in

$$P_2(dL|i) = \Pr\left(\sum_{j=1}^d \sum_{n=1}^L Z_{1nj} < \frac{dL}{2} | i\right). \quad (4.15)$$

There are a total of  $dL$  normalized outputs of branch 1 of the demodulator which corresponding to  $dL$  total hops. The random variables corresponding to all jammed hops are identically distributed as are all random variables corresponding to unjammed hops. For simplification of analysis, the  $n$  and  $j$  index of (4.15) are combined to one index,  $k$ , resulting in

$$P_2(dL|i) = \Pr\left(\sum_{k=1}^{dL} Z_{1k} < \frac{dL}{2} | i\right). \quad (4.16)$$

Let  $f_{Z_{1k}}^{(1)}(z_{1k})$  be the probability density function defined by (4.7) of  $z_{1k}$  assuming that hop  $k$  of  $dL$  hops has interference. Similarly, let  $f_{Z_{1k}}^{(2)}(z_{1k})$  be the probability density function of  $z_{1k}$  when hop  $k$  has no interference. Since the random variables corresponding with each hop are assumed to be independent, the conditional probability density of  $Z_1$  given that  $i$  of  $dL$  hops have interference is given as:

$$f_{Z_1}(z_1|i) = \left[ f_{Z_{1k}}^{(1)}(z_{1k}) \right]^{\otimes i} \otimes \left[ f_{Z_{1k}}^{(2)}(z_{2k}) \right]^{\otimes dL - i} \quad (4.17)$$

where  $\otimes i$  represents an  $i$ -fold convolution.

Now from the relationships of (4.16) and (4.17) we define

$$P_2(dL|i) = \int_0^{dL/2} f_{Z_1}(z_1|i) dz_1. \quad (4.18)$$

Equations (4.17) and (4.18) must be evaluated numerically. The result of (4.18) is then combined with (4.11) and (2.14) to obtain the union bound on the probability of bit error with soft decision decoding.

It can be seen that evaluation of the uncoded case requires  $r=1$  and  $d=1$  to obtain the conditional probability of bit error given  $i$  hops have interference as obtained in [Ref. 5]:

$$P_b(i) = \int_0^{L/2} f_{Z_1}(z_1|i) dz_1 \quad (4.19)$$

Equation (4.19) is then used in (3.2) to obtain the total uncoded probability of bit error.

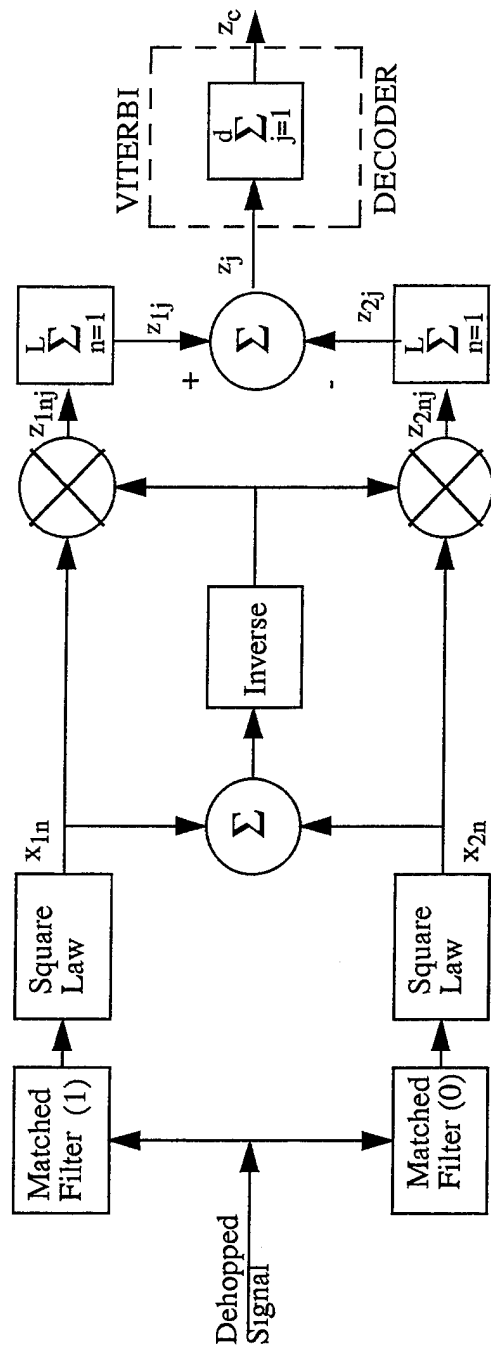


Figure 4.1: Model of FFH/BFSK Self-Normalized Receiver with Soft Decision Viterbi Decoding

## V. NUMERICAL ANALYSIS

Numerical analysis for this thesis was performed using MATLAB<sup>TM</sup>, an interactive system by The MathWorks Inc., designed for matrix and vector manipulation and general mathematical computations.

### A. NUMERICAL PROCEDURE

Computation of the bit error probability of the self-normalized receiver requires numerical computation of (4.17) and (4.18). Equation (4.17) requires discrete convolution while (4.18) requires numerical integration.

The random variable,  $Z_{1k}$ , representing the normalized hop output of the demodulator is limited to the range from 0 to 1. This limited range of the random variable makes numerical evaluation of the convolution straightforward. As stated in Brigham, for functions of finite interval, continuous convolution can be approximated by discrete convolution with an error no worse than that introduced by rectangular integration [Ref. 20]. However, solution of (4.17) using direct numerical convolution is extremely slow and involves a high number of computations. For computations involving higher levels of diversity and convolutional coding with soft decision decoding, a more efficient technique is required. For this reason, the Fast Fourier Transform (FFT), which is more computationally efficient, was used in this thesis to perform the discrete convolution.

The procedure was to evaluate the pdfs (4.7), (4.8) and (4.9) at fixed intervals,  $T$ , over their range. This provides a sampled version of each pdf. Next, the Discrete Fourier Transform of the pdf's to be convolved were calculated. The pdf's were then multiplied together term by term. The Inverse Discrete Fourier Transform (IDFT) is then calculated to obtain  $f_{Z_1}(z_1|i)$ .

After obtaining  $f_{Z_1}(z_1|i)$  over its range, the conditional probability of bit error  $P_2(dL|i)$  is obtained by evaluating (4.18) using Simpson's rule to approximate the continuous integral [Ref. 21].

The error involved in determining  $P_2(dL|i)$  is dependent upon a variety of factors. Error resulted from round-off error in the computer, error due to numerical integration, and aliasing of the sampled probability distribution functions. The probability of bit error was calculated for the range  $1 > P_b > 10^{-8}$ . Since, Matlab uses double-precision calculations, round-off error is negligible in this range. Errors resulting from aliasing of the pdf's and numerical integration were dependent upon the sampling or evaluation interval of the pdf's. Plots of the pdf (4.7), show that it is a relatively smooth function without abrupt variations in amplitude over its range. This fact suggests that a reasonable sampling interval can be found to give accurate results. The error due to numerical integration can be made as small as required by decreasing the sampling interval of the pdf. For errors due to both aliasing and integration, a smaller  $T$  results in smaller error but also increases the required number of computations and increases computation time.

Computation time and memory requirements become very large as  $d$  and  $L$  increase therefore making it necessary to find the largest possible sampling interval while still obtaining accurate results. It was found that there was no difference in the plotted results, for a probability of bit error varying from 1 to  $10^{-8}$ , when  $T$  was as large as 1/100 or as small as 1/1000. These results indicate that aliasing and integration error were negligible in this range and  $T$  was set at 1/100.

Since a closed form solution for the system's probability of bit error is not attainable, it is impossible to determine the exact error in calculations. Therefore, as a check on the accuracy of results, probability of bit error was calculated for the system without coding. Performance in the uncoded case matches previous documented results [Ref. 4] and [Ref. 5] where different techniques for performance analysis were utilized.

System performance is evaluated for various values of fraction of bandwidth jammed,  $\gamma$ , diversity and fading conditions. Constraint lengths and code rates were varied to determine their effects. Constant bit energy and constant hop energy systems were evaluated. Two cases of total spread bandwidth were also examined. In one case, the spread bandwidth was assumed to be constrained. In the second case, the bandwidth was assumed to increase with increasing diversity and with the addition of convolutional coding.

The number of frequency hop bins was fixed at  $N=1000$ . Worst case fractions of the bandwidth jammed,  $\gamma_{wc}$ , were obtained numerically by evaluating the probability of bit error vs.  $E_b/N_f$  with fifteen different values of  $\gamma$ , logarithmically spaced from the maximum value of 1 (barrage jamming) to a minimum of  $1/N$ . The maximum of the 15 values of  $P_b$  at each value  $E_b/N_f$  then represented worst case performance.

For purposes of this thesis, numerical results were obtained for diversities of  $L = 2, 3, 4$  and for no diversity ( $L=1$ ). The code rates examined were  $r=1/2$  and  $r = 1/3$  with the constraint lengths varying from 3 to 9.

### 1. Constant Bit Energy and Constant Spread Bandwidth

Previous analysis of FFH/BFSK systems have typically held the spread bandwidth constant as diversity and coding were added to the system [Ref. 22]. The total spread bandwidth,  $W$ , as defined in Chapter II is proportional to  $NR_h=NB$ . For a constant energy per bit system, the hop rate increases by a factor of  $1/r$  and  $L$  with the additions of coding and diversity respectively. If  $W$  is held constant, then it is assumed that the number of hopping frequencies,  $N$ , decreases. Defining the bandwidth of a frequency bin without coding or diversity as  $B$ , and the bandwidth of a system with diversity  $L$  and code rate,  $r$ , as  $B'$ , then we have the relationship  $B' = LB/r = LR_h/r$ .

The signal power-to-noise power ratio is related to  $E_b/N_T$  by:

$$\frac{S}{\sigma_k^2} = \frac{S}{\left[N_o + \frac{N_I}{\gamma}\right]B'} = \frac{(rS)/(LB)}{N_o + \frac{N_I}{\gamma}} = \frac{rE_h/L}{N_o + \frac{N_I}{\gamma}} = \left(\frac{r}{L}\right) \frac{E_h}{N_T}. \quad (5.1)$$

The relationship shows that the ratio of signal power to noise power decreases with increasing diversity and with the addition of convolutional coding.

## 2. Constant Hop Energy and Varying Spread Bandwidth

For the case of a constant signal energy per hop system we assume that the information data rate decreases with increasing diversity. The bandwidth of a frequency bin thus does not increase with increasing diversity. To fairly compare coded and uncoded performance at a constant data rate, we assume that the frequency bin bandwidth increases by the factor  $1/r$  with the addition of coding. If the number of frequency hopping bins remains constant then the total spread bandwidth must expand. We thus have the relationships  $B' = B/r$  and

$$\frac{S}{\sigma_k^2} = \frac{S}{\left[N_o + \frac{rN_I}{\gamma}\right]B'} = \frac{rS/B}{N_o + \frac{rN_I}{\gamma}} = \frac{rE_h}{N_o + \frac{rN_I}{\gamma}}. \quad (5.2)$$

This relationship shows that the signal power-to-noise power ratio remains constant with increasing diversity but is decreased by a factor of  $r$  with the addition of convolutional coding when thermal noise is significant.

## 3. Constant Bit Energy and Varying Spread Bandwidth Systems

In this analysis,  $N$  was assumed to be held constant and the bandwidth of a frequency bin,  $B' = LB/r$ , expands with increasing diversity and the use of coding. Since the jammer is power limited, the power spectral density of the jammer interference becomes  $(rN_I)/(\gamma L)$ . The signal power-to-noise power ratio is related to the hop energy to total noise interference power spectral density by:

$$\frac{S}{\sigma_k^2} = \frac{S}{\left[N_o + \frac{rN_I}{\gamma L}\right]B'} = \frac{(rS)/(LB)}{N_o + \frac{rN_I}{\gamma L}} = \frac{rE_h/L}{N_o + \frac{rN_I}{\gamma L}}. \quad (5.3)$$

If thermal noise is assumed to be negligible then (5.2) and (5.3) are equivalent.

The ratio of direct-to-diffuse signal power,  $\eta$ , was assumed to be the same for each hop  $k$  of the bit. The value of  $\eta$ , was varied from 0 for Rayleigh fading to 1 for a weak direct signal, 10 for a strong direct signal, and infinite for the no fading case.



## VI. NUMERICAL RESULTS AND DISCUSSION

In Figures 6.1-6.11 we assume constant bit energy and constant spread bandwidth systems. The plots shown in Figures 6.1, 6.2 and 6.3 compare probability of bit error as a function of  $E_b/N_I$  for the self-normalized receiver with no diversity. Performance with convolutional coding and soft decision decoding is compared against uncoded performance. The three classes of fading are Rayleigh fading, Rician fading with a strong direct signal ( $\alpha^2/2\sigma^2=10$ ), and a nonfading channel. The jammer is assumed to perform worst case partial-band jamming. Convolutional coding with soft decision Viterbi decoding is observed to improve performance when  $E_b/N_I$  is greater than 15 dB (Fig. 6.1), 10 dB (Fig. 6.2), and 8 dB (Fig. 6.3) and  $E_b/N_0$  is equal to 13.35 dB. In Figure 6.3 where the channel is nonfading, the convolutional coding changes the relationship between the probability of bit error and  $E_b/N_I$  from a linear relationship to an exponential relationship. The constraint lengths of the convolutional codes used are 3,5,7 and 9. In all cases of fading, the coding gains increase as the constraint length of the convolutional code is increased. For example, for the Rician fading case ( $\alpha^2/2\sigma^2=10$ ) of Fig. 6.2, at  $P_b=10^{-5}$ , we see an approximate 10 dB coding gain for the largest constraint length code ( $v=9$ ) over the smallest constraint length code ( $v=3$ ).

A comparison of the effectiveness of worst case partial-band jamming over barrage jamming, for various constraint lengths ( $v=3, 9$ ) of codes with soft decision decoding and with no coding is shown in Figures 6.4 and 6.5 for Rician fading ( $\alpha^2/2\sigma^2=10$ ) and nonfading channels, respectively. When the system is uncoded and without diversity, partial-band jamming is much more detrimental to the system performance of the self-normalized receiver than is barrage jamming. We expect this result since the uncoded performance of the self-normalized receiver without diversity is equivalent to that of the conventional receiver. When the system uses convolutional coding and soft decision decoding, the differences between worst case partial-band jamming and barrage jamming

decrease. Convolutional coding is seen to drive the jammer towards a barrage jamming strategy. In addition, the relative effectiveness of worst case partial-band jamming over barrage jamming decreases as the constraint length of the code is increased. This result indicates that by using a convolutional code with a high enough constraint length, the partial-band jammer can be totally defeated. Since there is a present practical limit to constraint length size, the convolutional coding can be made more powerful by using it in combination with repetition coding or diversity. Figure 6.6 shows that when diversity of  $L=2$  or greater is used in conjunction with convolutional coding and soft decision decoding, that even with the weakest constraint length code,  $v=3$ , the jammer is driven to barrage jamming when  $E_b/N_0$  is equal to 13.35 dB.

The difference in effectiveness of worst case partial-band jamming over barrage jamming is also dependent upon the ratio of  $\alpha^2/2\sigma^2$ . For a Rayleigh fading channel, previous analysis has shown that barrage jamming is worst case when the system is uncoded [Ref. 5]. Barrage jamming is also worst case when the system contains convolutional coding. This result, and comparison of Fig. 6.4 and Fig 6.5, indicate that the relative effectiveness of partial-band jamming over barrage jamming increases as  $\alpha^2/2\sigma^2$  increases.

Previous works analyzing the uncoded performance of the self-normalized receiver have shown a clear advantage to increasing diversity to combat the effects of partial-band jamming and of multipath fading. The effects of increasing diversity in conjunction with convolutional coding and soft decision decoding was examined for various fading channels. Figure 6.7 shows performance for a Rician fading channel with a weak direct signal. When  $E_b/N_I$  is less than 20 dB and  $E_b/N_0$  is equal to 13.35 dB, the performances for diversity levels of  $L=1,2,3,4$  are roughly equivalent. In this range of  $E_b/N_I$ ,  $L=2$  gives the best performance providing approximately a 2 dB advantage over the worst performance of  $L=4$ . For  $E_b/N_I$  greater than 20 dB use of diversity levels of 2,3 and 4 are far superior over the use no diversity. The optimal level of diversity of 3 shows an asymptotic

probability of bit error below  $10^{-4}$  while for  $L=1$  the asymptotic limit is above  $10^{-3}$ . Figure 6.8 shows the probability of bit error for increasing diversity in a nonfading channel. For a code constraint length of three, performance degrades as diversity increases for diversity levels greater than two. For high and low  $E_b/N_I$ ,  $L=1$  is superior to  $L=2$ . If a stronger constraint length code ( $v=9$ ) is used, as shown in Fig. 6.9, diversity provides no advantage. Figure 6.10 shows that the result in a fading channel with a strong direct signal ( $\alpha^2/2\sigma^2=10$ ) is similar. Increasing diversity in a constant energy per bit system with a constrained spread bandwidth results in the combining of an increasing number of hops per bit and a corresponding increase in combining losses. The combining losses are worsened since the ratio  $E_b/N_I$  decreases with increasing  $L$ . The same is not true for increasing constraint length since  $E_b/N_I$  remains constant as the free distance,  $d_{free}$ , of the code increases. When using a soft decision decoder and a convolutional code with a constraint length of nine, the use of diversity degrades performance.

In Fig 6.11 we examine the effect that the signal-to-thermal noise ratio has on system performance. Figure 6.11 examines the coded and uncoded performance of a system for a fading channel with  $\alpha^2/2\sigma^2$  equal to 10 and  $E_b/N_o$  now raised to 16 dB. We first note that the use of coding improves performance at a lower level of  $E_b/N_I$  than noted in Fig. 6.4. For a constraint length equal to nine, coded performance is superior to uncoded performance at  $E_b/N_I$  equal to 9 dB. By comparing coded performance with a constraint length equal to 3 in Fig. 6.4 and 6.11, we also see that the relative effectiveness of partial-band jamming over barrage jamming is increased as  $E_b/N_o$  increases. As thermal noise lessens, the signal becomes less degraded. More jammer power per hop is thus required to degrade the signal and cause errors. The jammer thus jams only a fraction of the bandwidth to increase the jammer power per hop for jammed hops.

In Figures 6.12-6.15 we allow the spread bandwidth to expand with increasing diversity for a constant energy per bit system and with the addition of coding to the system. When a constant energy per hop system is used, performance improves with increasing

diversity. Figure 6.12 shows performance in a Rician fading channel with soft decision decoding, with diversity of  $L=1,2,3,4$ . The increase in diversity effectively increases the bit energy-to-interference ratio. For  $P_b$  equal to  $10^{-7}$ , we see a diversity gain of approximately 13 dB through the use of  $L=4$  over no diversity. The disadvantage of this method is that the data rate has been decreased by a factor of  $L$ . Performance approaching that of a constant energy per hop system without decreasing the data rate can be obtained with a constant energy per bit system if the spread bandwidth is allowed to increase with diversity. If the spread bandwidth,  $W$ , is not constrained then the number of hopping frequencies can remain constant as diversity increases. The increase in the spread bandwidth,  $W$ , forces the jammer to spread its power over a much wider bandwidth. As the signal-to-thermal noise ratio increases the performance of this system approaches that of a constant energy per hop system. Figure 6.13 shows that when the spread bandwidth is allowed to expand with increasing diversity and  $E_b/N_0$  is equal to 13.35 dB, the use of diversity begins to show some advantage. In this case, diversity levels of 2,3 and 4 all provide superior performance over no diversity. A diversity level of 2 however provides superior performance over  $L=3$  and 4 which can be attributed to the effect of thermal noise on combining losses. The additional spreading of the bandwidth is equivalent to keeping the ratio  $E_b/N_f$  constant. The ratio  $E_b/N_0$ , however, decreases with increasing diversity as in the constrained bandwidth case since the thermal noise is not bandlimited. Fig. 6.14 shows the performance of another constant energy per hop system while Fig. 6.15 shows a constant energy per bit system with a varying bandwidth. Both of these systems have a higher  $E_b/N_0$  than in the previous example. In Fig. 6.15, we see that by increasing  $E_b/N_0$  to the large level of 20 dB where thermal noise becomes less of a factor, the trend of improved performance with increasing diversity results as in the constant energy per hop case. It can be seen, as expected, that the performance with a constant energy per hop in Fig. 6.14 is nearly identical to the performance shown in Fig. 6.15.

Hard and soft decision decoding are compared in Figures 6.16 and 6.17 for the nonfading and Rayleigh fading cases. For these results a constant bit energy and spread bandwidth is assumed. In a nonfading channel for a probability of bit error of  $10^{-7}$ , soft decision decoding is superior to hard decision decoding by 4-5 dB for code rates of  $r=1/3$  and  $r=1/2$  and constraint length 7. In the Rayleigh fading case, soft decision decoding is also superior. The hard decision decoder is unable to use the side information available at the output of the self-normalized receiver. This side information is utilized by the soft decision decoder which provides a significant performance advantage.

Figures 6.18 and 6.19 compare performance with soft decision decoding of the self-normalized receiver and conventional receiver with perfect side information assuming a constant bit energy and spread bandwidth. In Figure 6.18 when  $E_b/N_0$  is greater than  $E_b/N_I$  the receiver with perfect side information is superior by 1-2 dB. As  $E_b/N_I$  increases the receiver with perfect side information drops jammed hops even though the relative jammer power per hop is very small. Since thermal noise is not negligible, the small gain achieved by dropping jammed hops is outweighed by the large degradation due to thermal noise. The conventional receiver with perfect side information reaches a noise floor on performance directly related to the signal to thermal noise ratio. This noise floor as shown in Fig. 6.18 occurs when  $E_b/N_I$  is less than  $E_b/N_0$ .

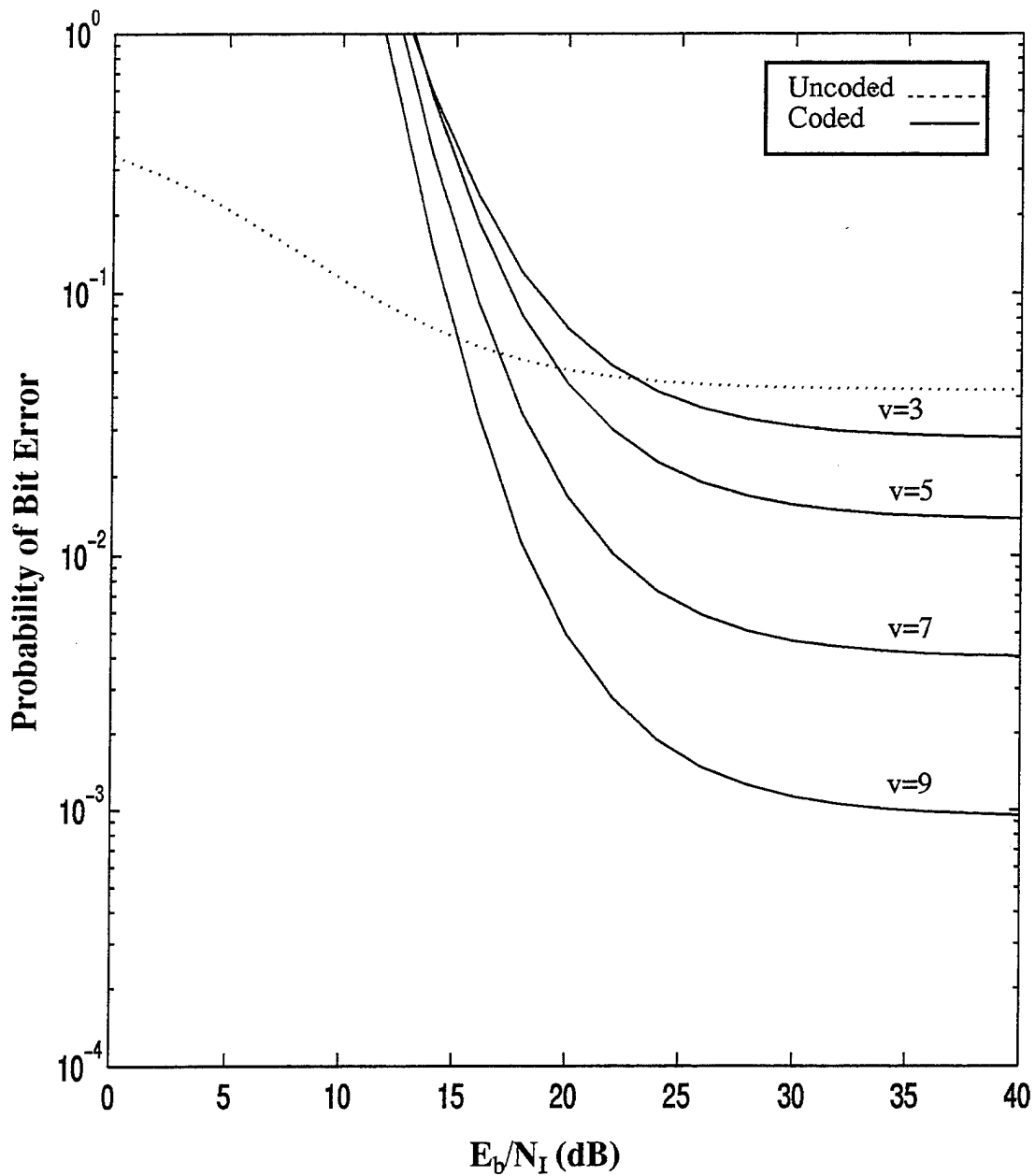


Figure 6.1: Uncoded and coded performance of the self-normalized receiver with worst case partial-band jamming, Rayleigh fading, with  $E_b/N_o = 13.35$  dB,  $L=1$  and soft decision Viterbi decoding with  $r=1/2$  and constraint lengths of 3,5,7, and 9.

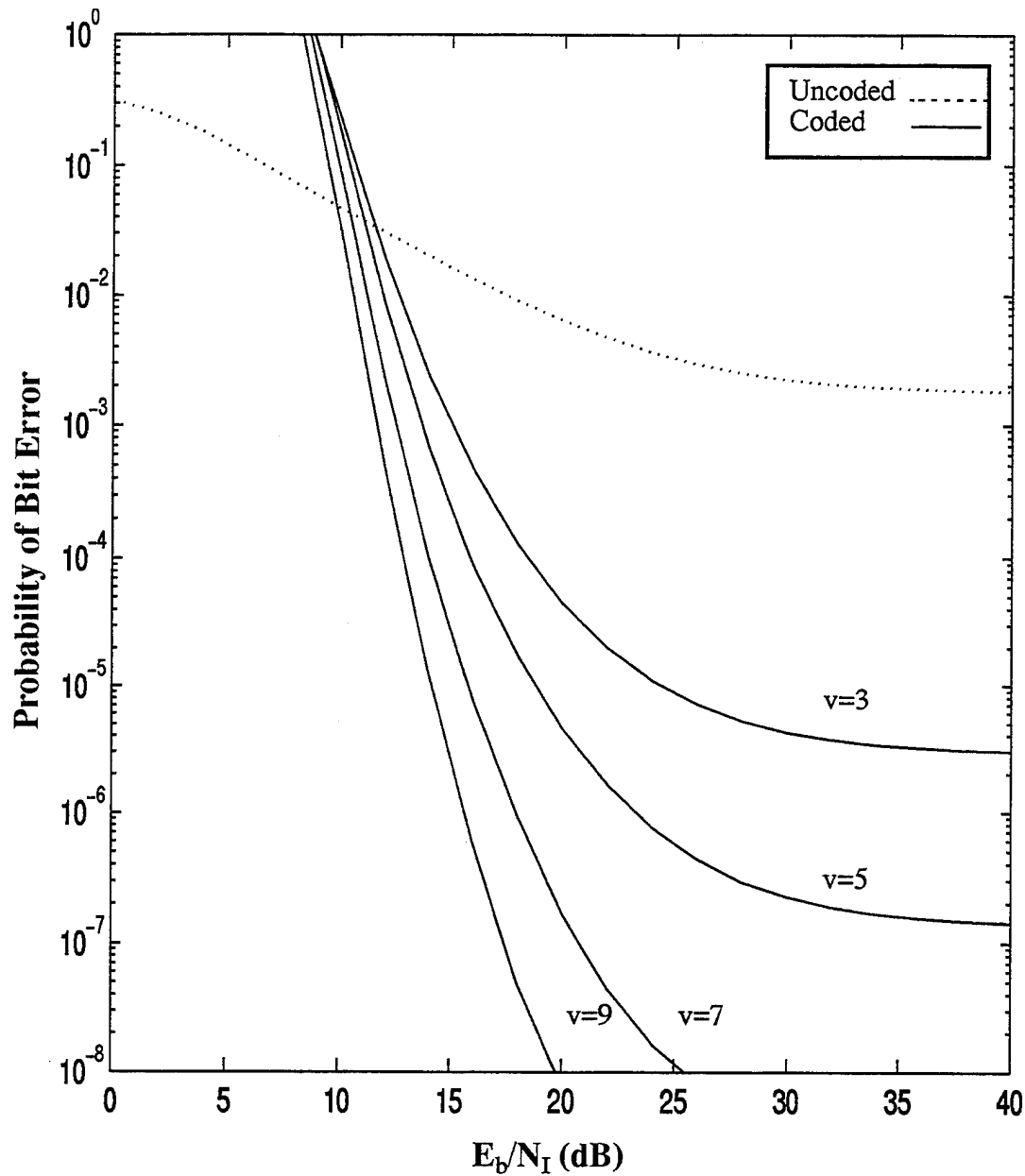


Figure 6.2: Uncoded and coded performance of the self-normalized receiver with worst case partial-band jamming, Rician fading and strong direct signal,  $\alpha^2/2\sigma^2=10$ , with  $E_b/N_o=13.35$  dB,  $L=1$  and soft decision Viterbi decoding with  $r=1/2$  and constraint lengths of 3,5,7, and 9.

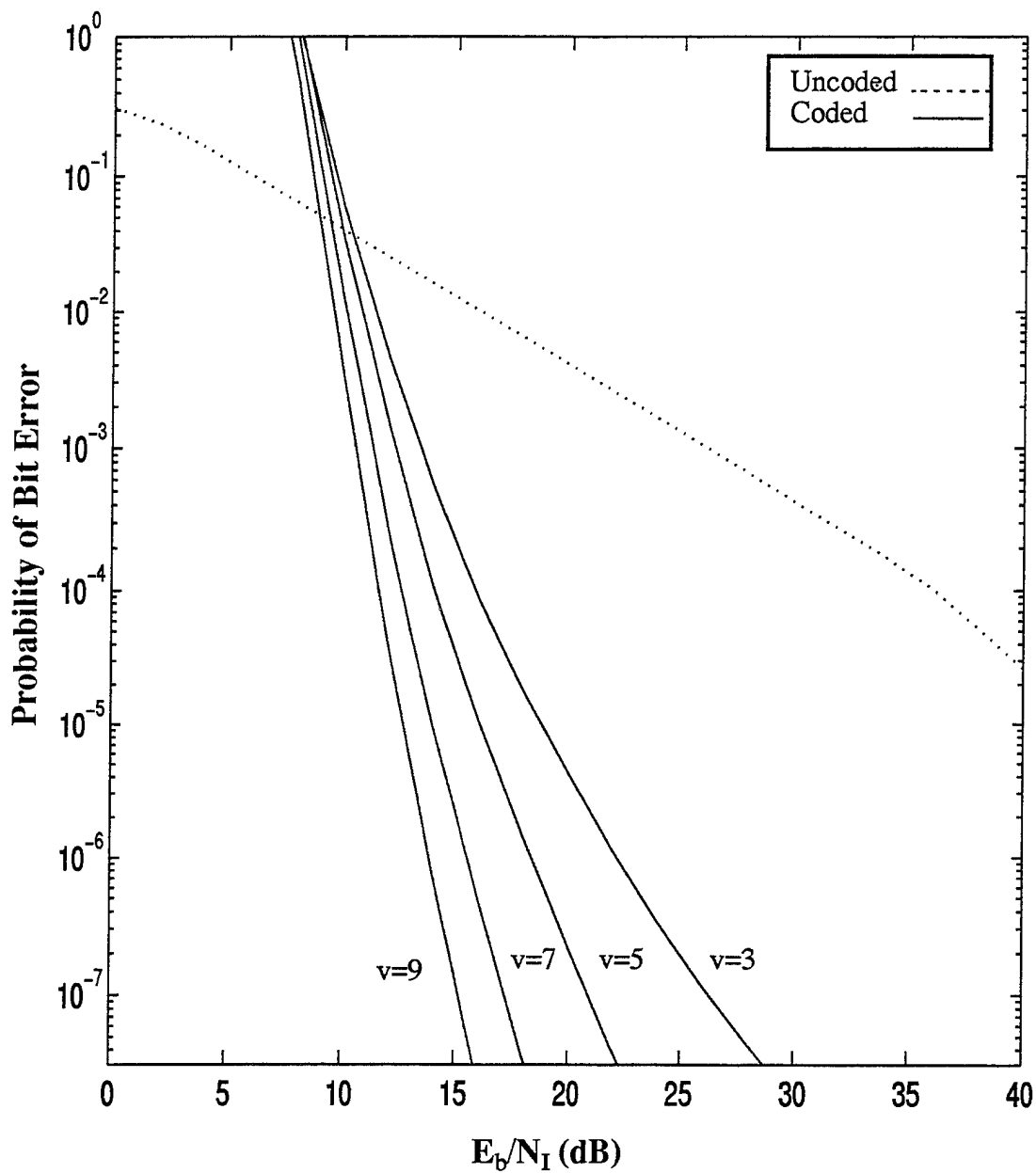


Figure 6.3: Uncoded and coded performance of the self-normalized receiver with worst case partial-band jamming, no fading, with  $E_b/N_0=13.35$  dB,  $L=1$  and soft decision Viterbi decoding with  $r=1/2$  and constraint lengths of 3,5,7, and 9.

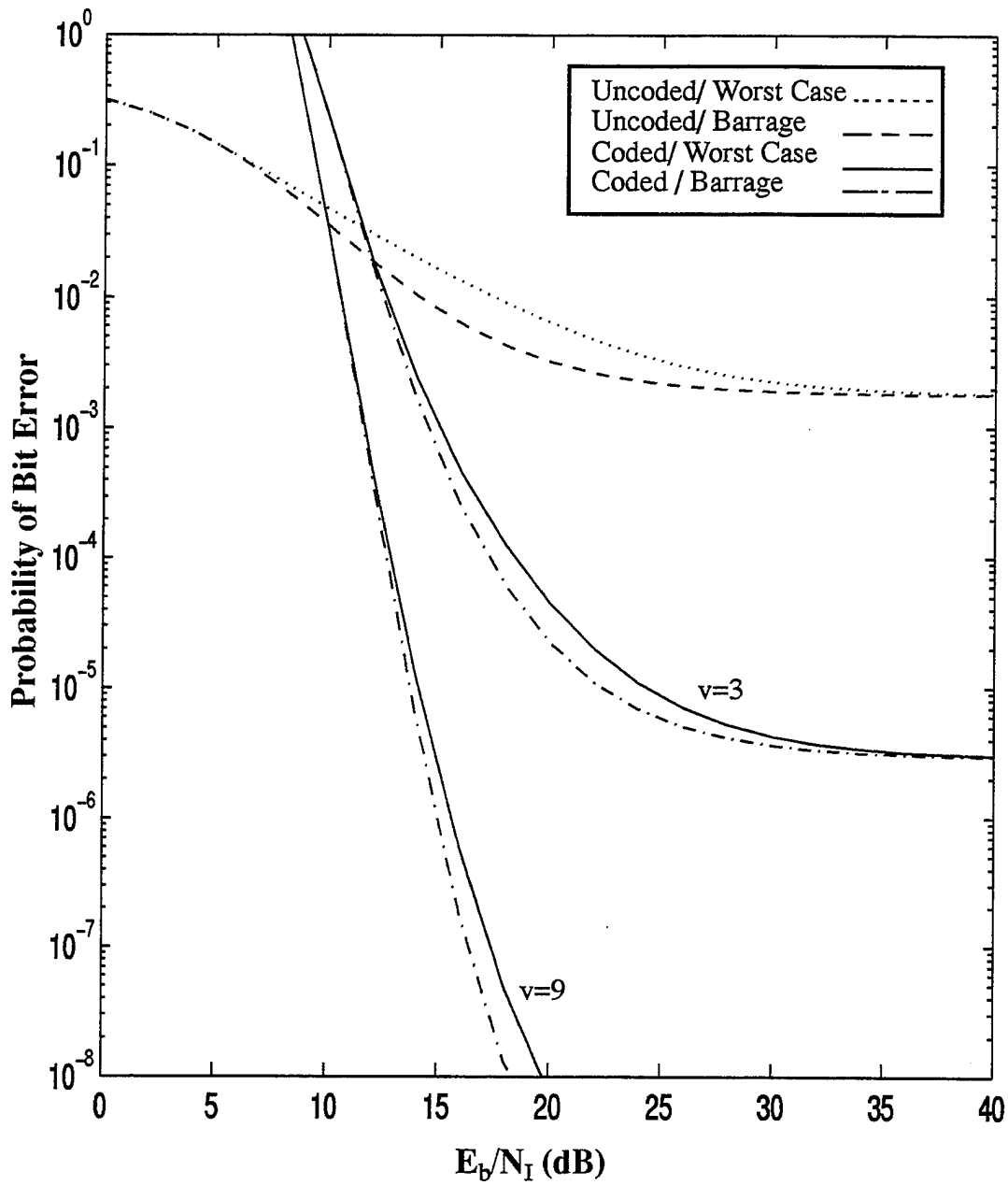


Figure 6.4: Uncoded and coded performance of the self-normalized receiver with worst case partial-band and barrage jamming, Rician fading and strong direct signal,  $\alpha^2/2\sigma^2=10$ , with  $E_b/N_o=13.35$  dB,  $L=1$  and soft decision Viterbi decoding with  $r=1/2$  and constraint lengths 3 and 9.

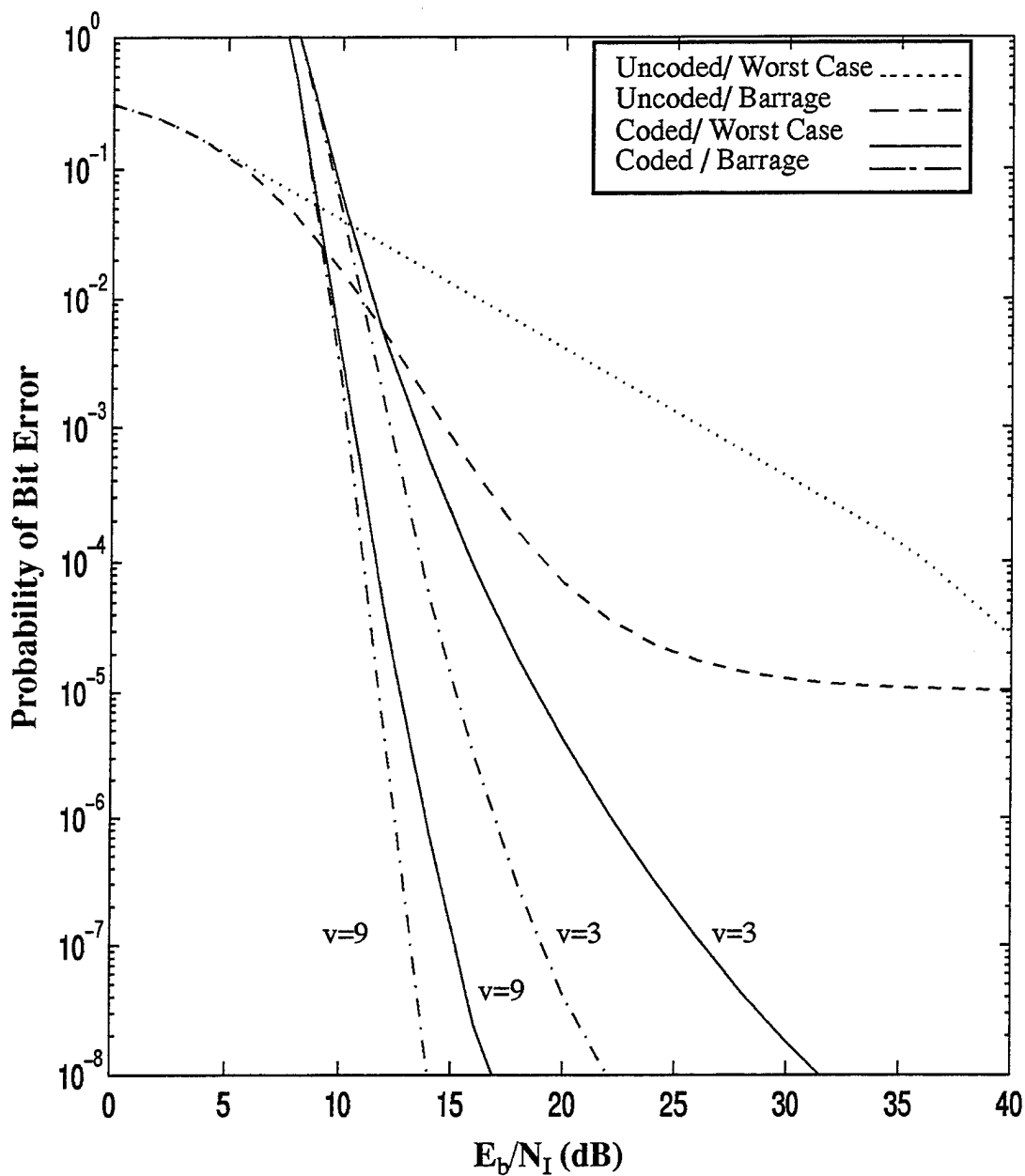


Figure 6.5: Uncoded and coded performance of the self-normalized receiver with worst case partial-band and barrage jamming, no fading with  $E_b/N_0 = 13.35$  dB,  $L=1$  and soft decision Viterbi decoding with  $r=1/2$  and constraint lengths 3 and 9.

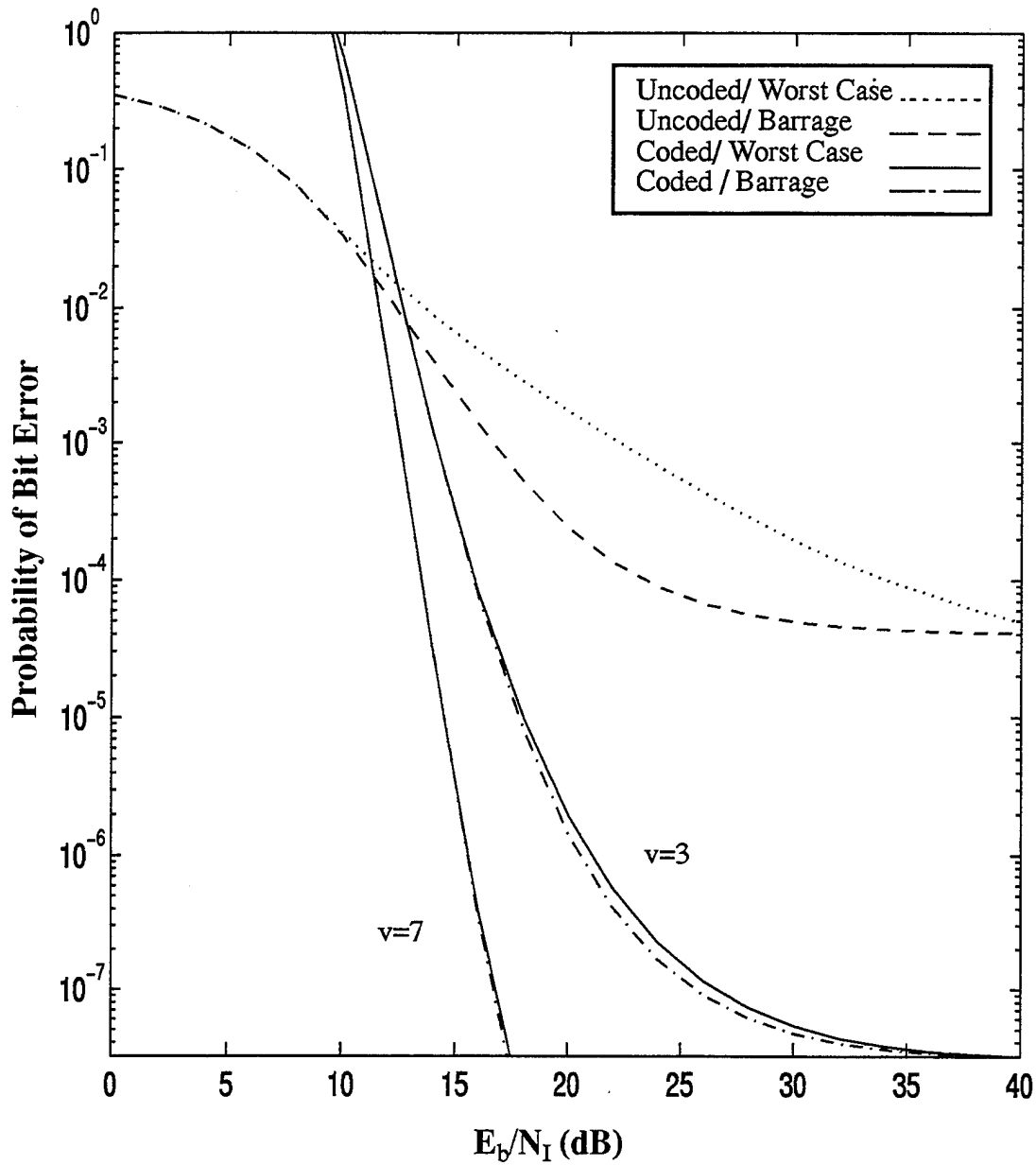


Figure 6.6: Uncoded and coded performance of the self-normalized receiver with worst case partial-band and barrage jamming, no fading, with  $E_b/N_o = 13.35$  dB,  $L=2$  and soft decision Viterbi decoding with  $r=1/2$  and constraint lengths of 3 and 9.

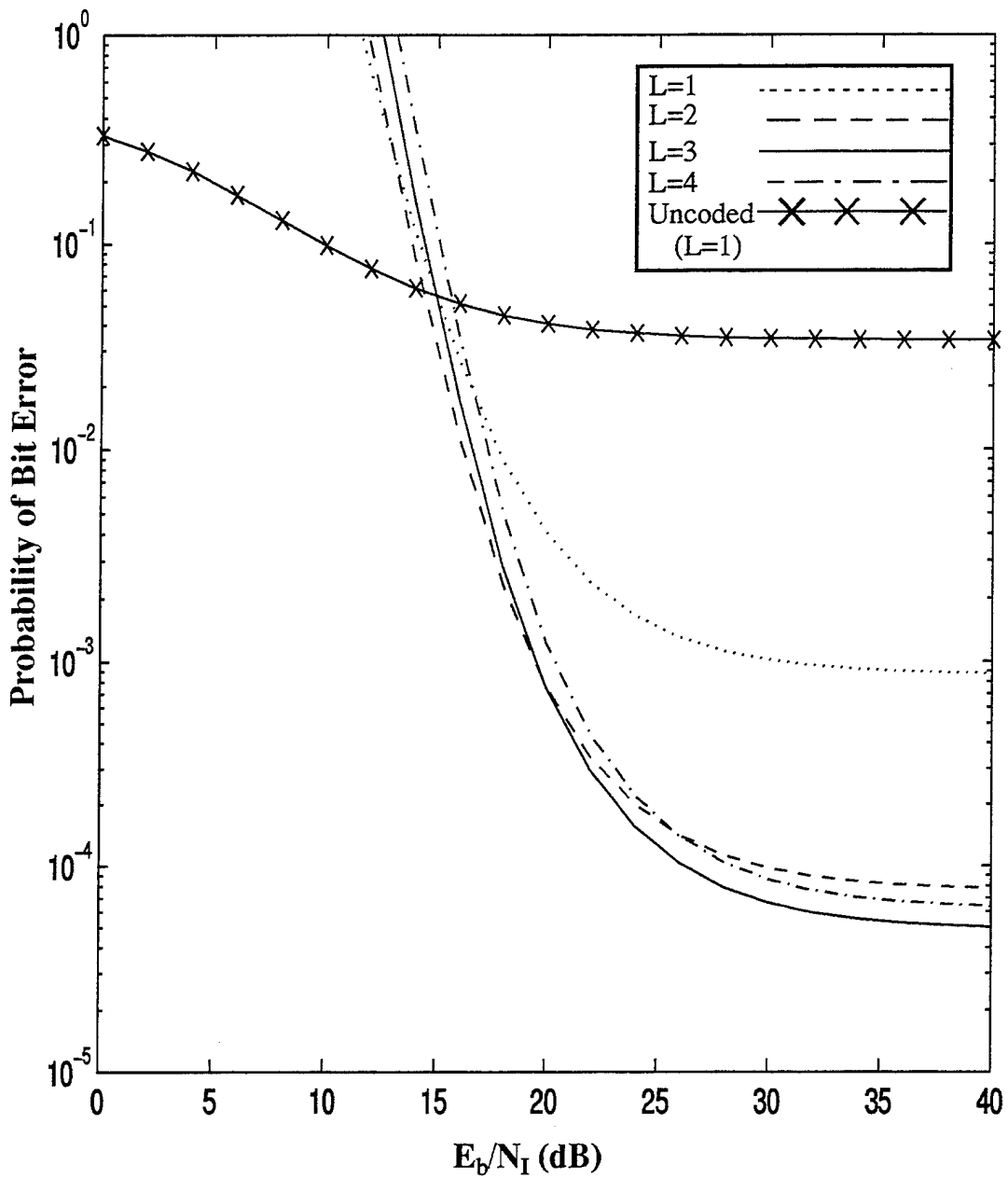


Figure 6.7: Performance of the self-normalized receiver with worst case partial-band jamming, Rician fading and weak direct signal,  $\alpha^2/2\sigma^2=1$ , with  $E_b/N_0 = 13.35$  dB,  $L=1,2,3$  and 4 and soft decision Viterbi decoding with  $r=1/2$  and constraint length 7.

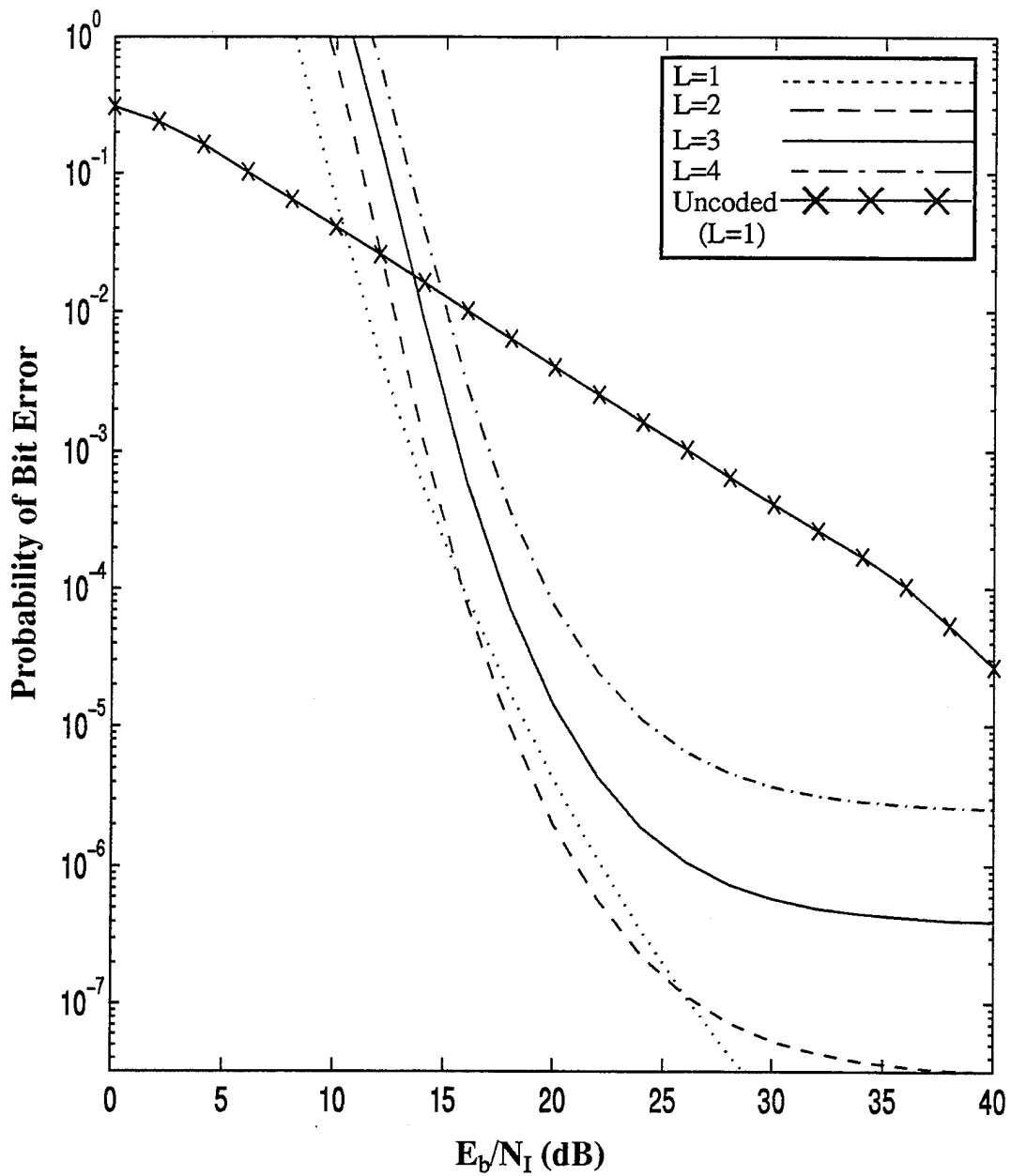


Figure 6.8: Performance of the self-normalized receiver with worst case partial-band jamming, no fading, with  $E_b/N_0 = 13.35$  dB,  $L=1,2,3$  and 4 and soft decision Viterbi decoding with  $r=1/2$  and constraint length 3.

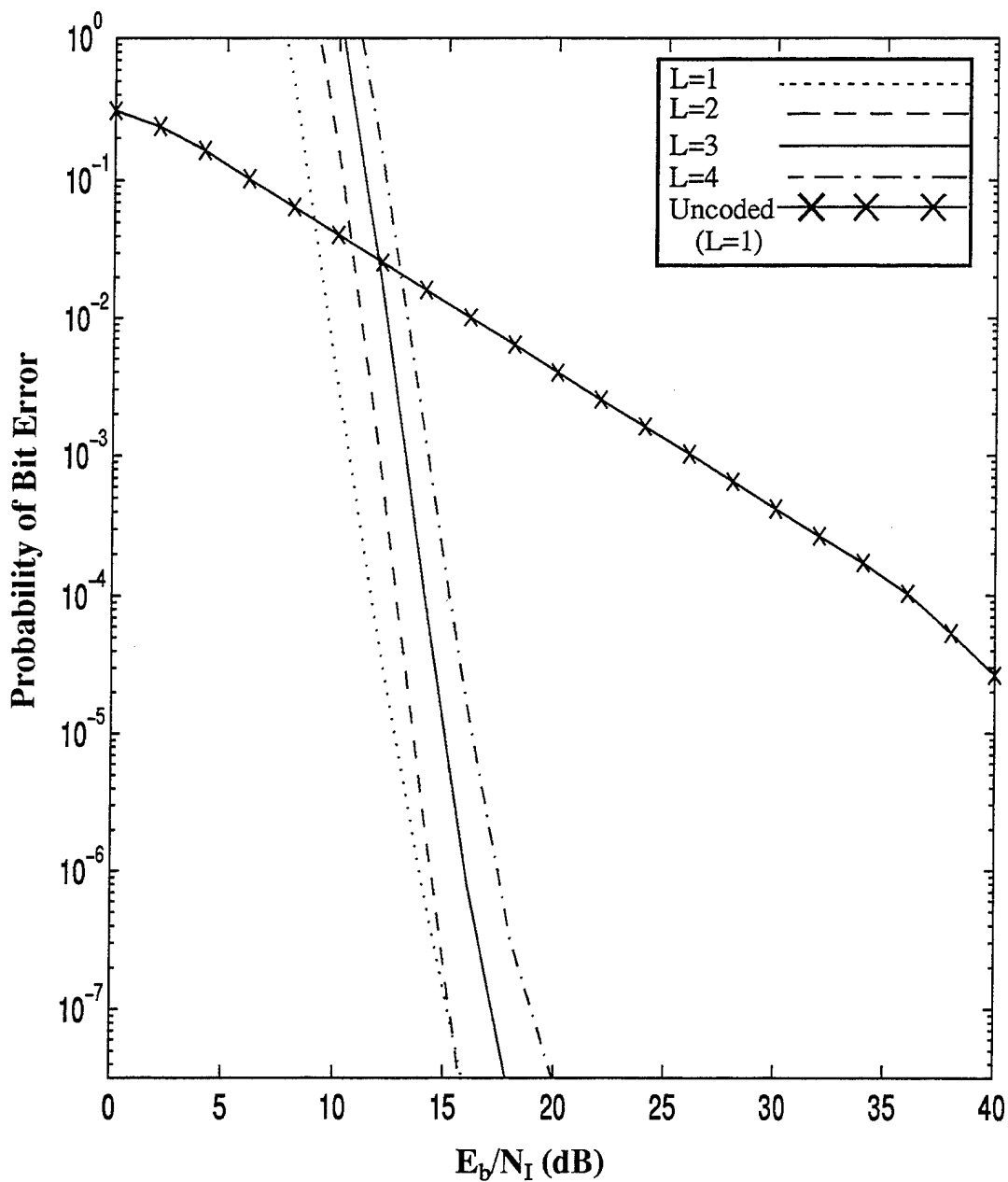


Figure 6.9: Performance of the self-normalized receiver with worst case partial-band jamming, no fading, with  $E_b/N_0 = 13.35$  dB,  $L=1, 2, 3$  and 4 and soft decision Viterbi decoding with  $r=1/2$  and constraint length 9.

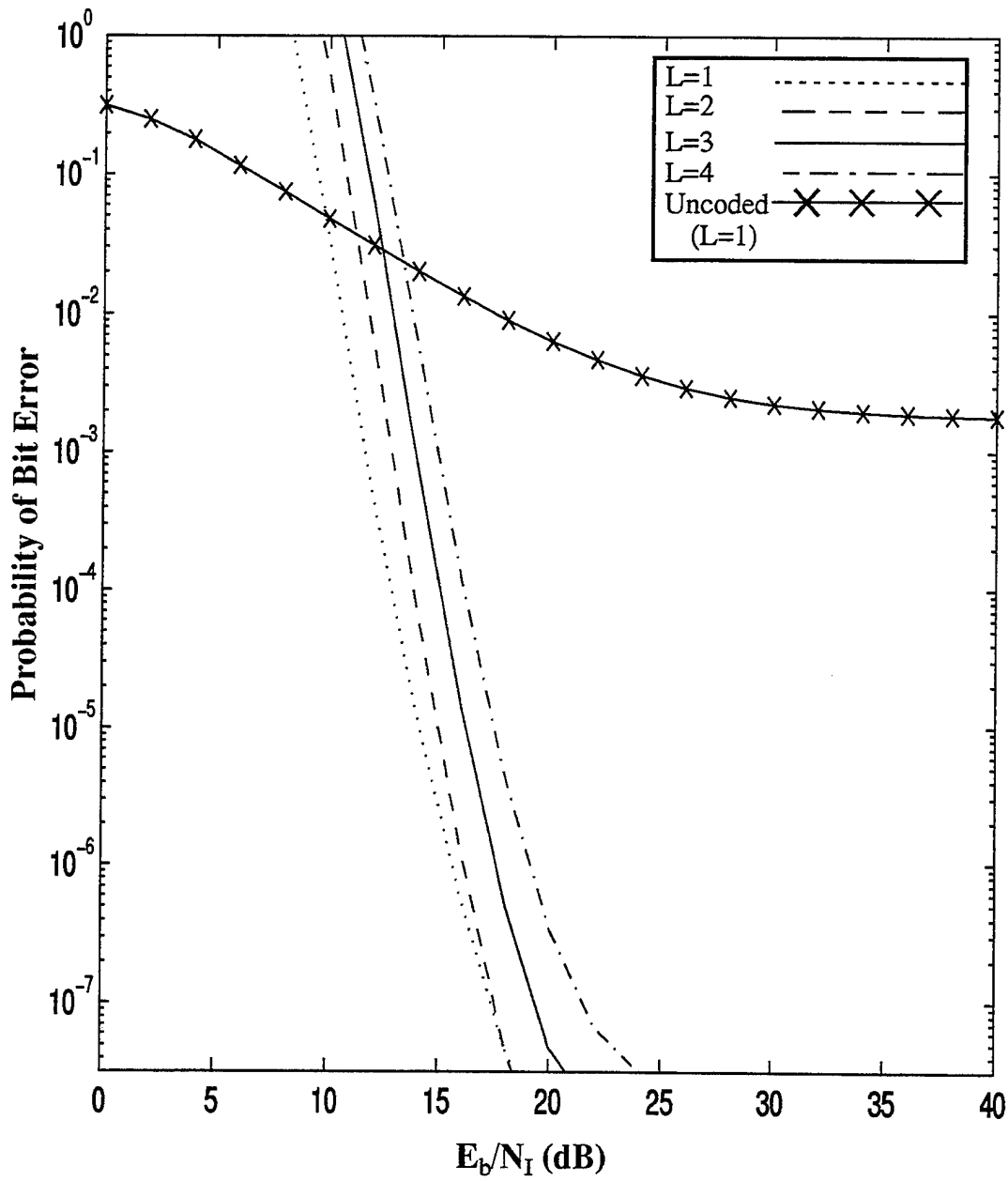


Figure 6.10: Performance of the self-normalized receiver with worst case partial-band jamming, Rician fading and strong direct signal,  $\alpha^2/2\sigma^2=10$ , with  $E_b/N_0=13.35$  dB,  $L=1,2,3$  and 4 and soft decision Viterbi decoding with  $r=1/2$  and constraint length 9.

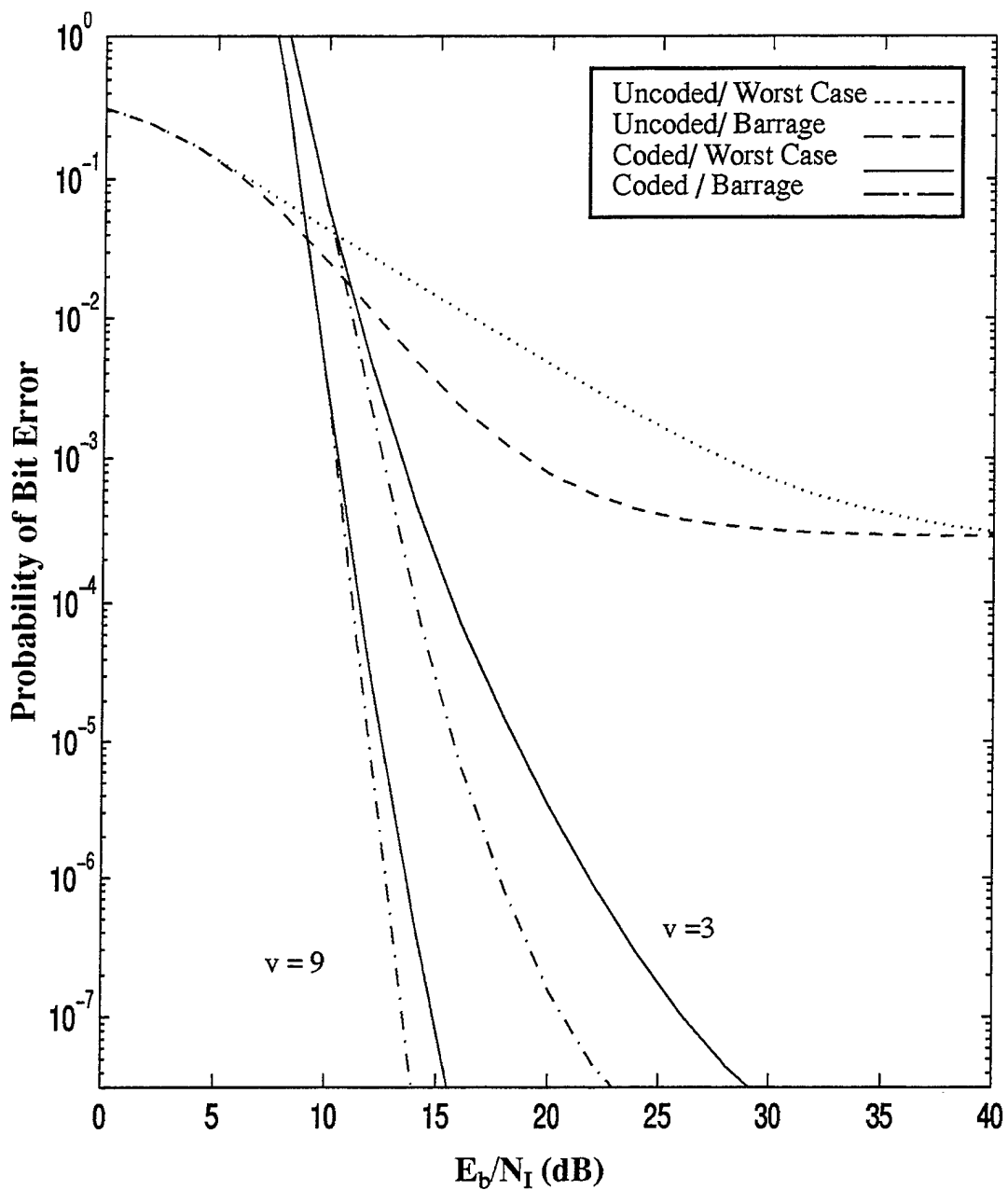


Figure 6.11: Uncoded and coded performance of the self-normalized receiver with worst case partial-band and barrage jamming, Rician fading and strong direct signal,  $\alpha^2/2\sigma^2=10$ , with  $E_b/N_0 = 16$  dB,  $L=1$  and soft decision Viterbi decoding with  $r=1/2$  and constraint lengths 3 and 9.

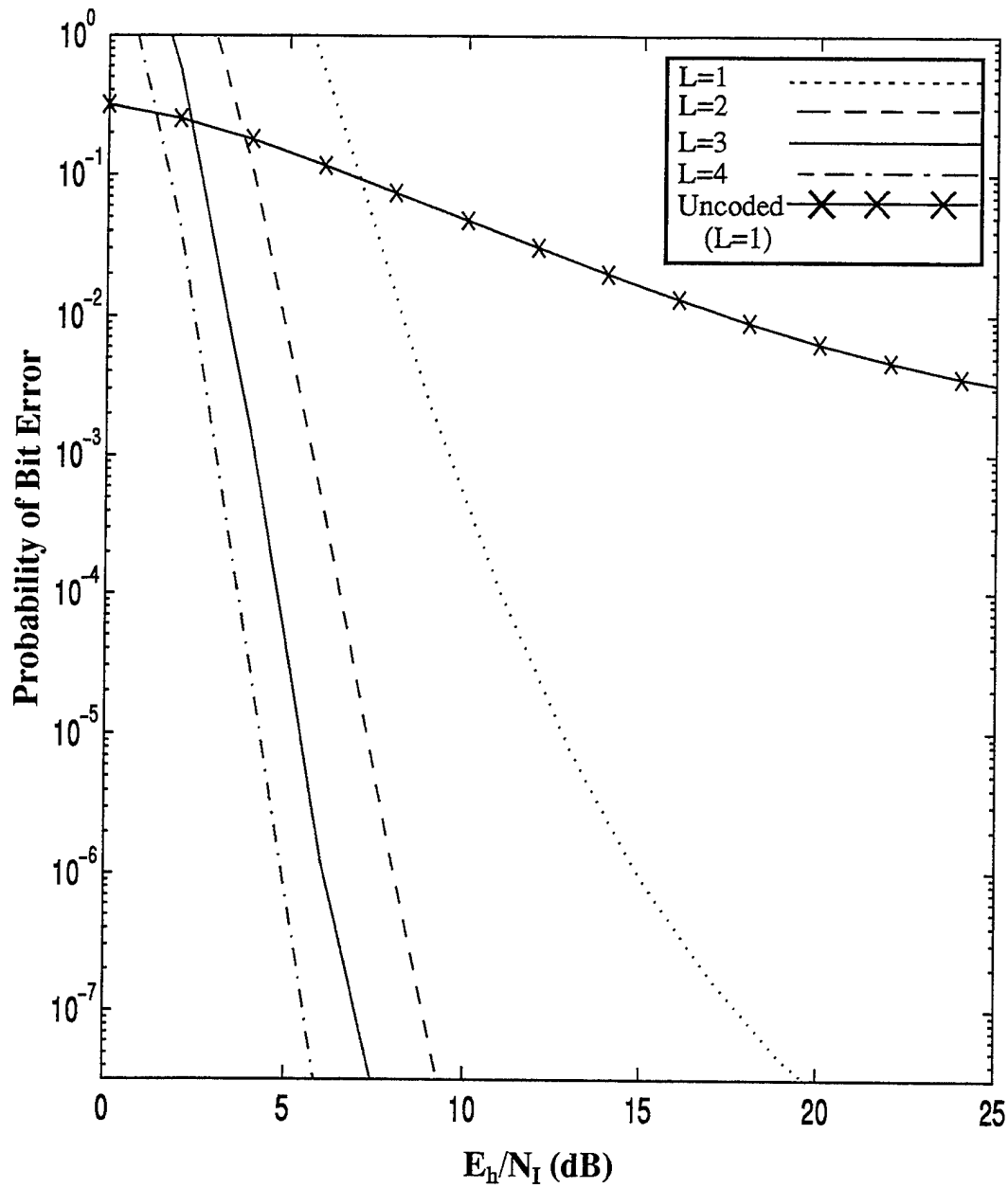


Figure 6.12: Performance of the self-normalized receiver with worst case partial-band jamming, Rician fading and strong direct signal,  $\alpha^2/2\sigma^2=10$ , with  $E_b/N_0=13.35$  dB,  $L=1,2,3$  and 4 and soft decision Viterbi decoding with  $r=1/2$  and constraint length 7 under assumption of constant energy per hop and varying spread bandwidth.

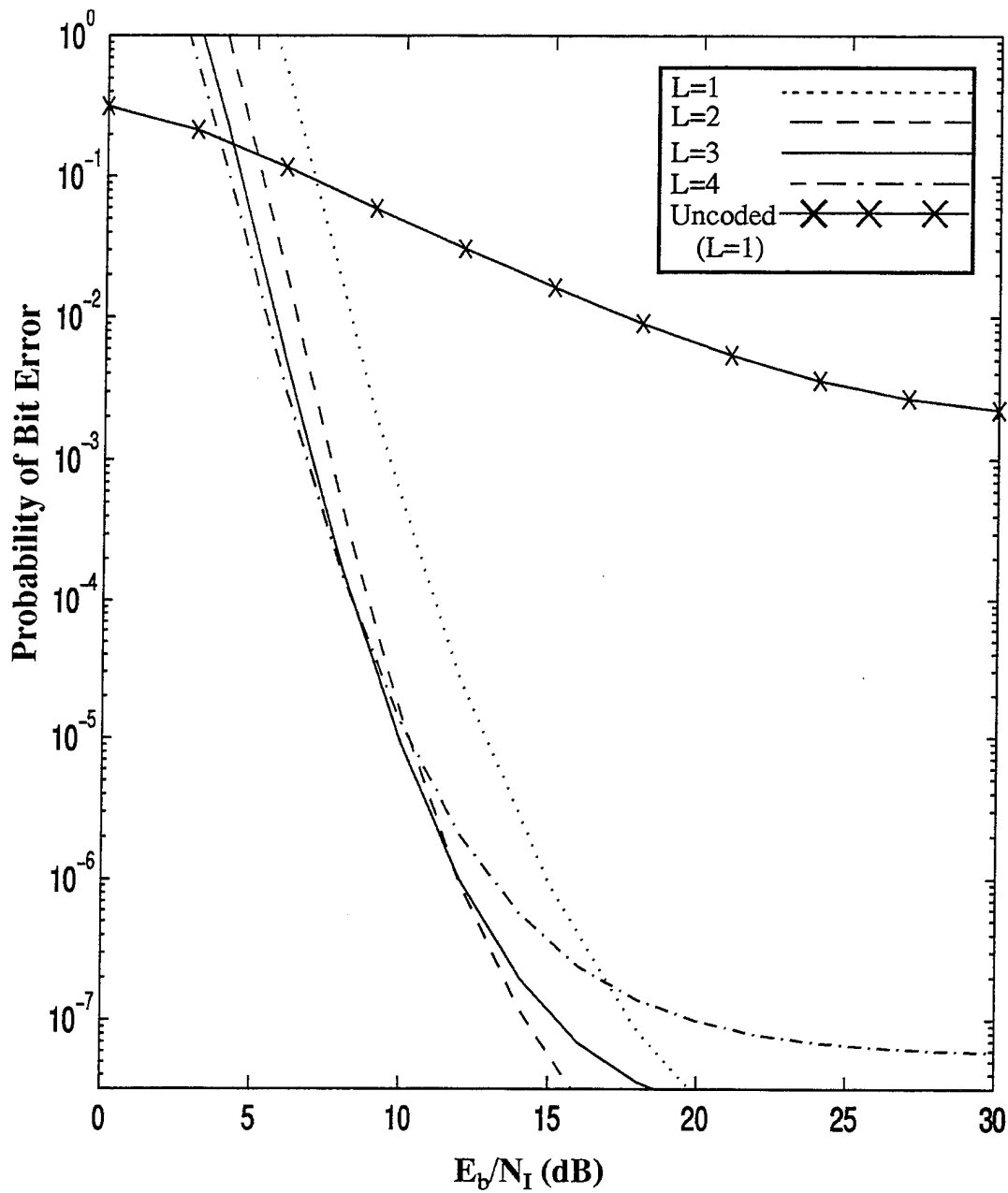


Figure 6.13: Performance of the self-normalized receiver with worst case partial-band jamming, Rician fading and strong direct signal,  $\alpha^2/2\sigma^2=10$ , with  $E_b/N_0=13.35$  dB,  $L=1,2,3$  and 4 and soft decision Viterbi decoding with  $r=1/2$  and constraint length 7 and under assumption of constant energy per bit and varying spread bandwidth.

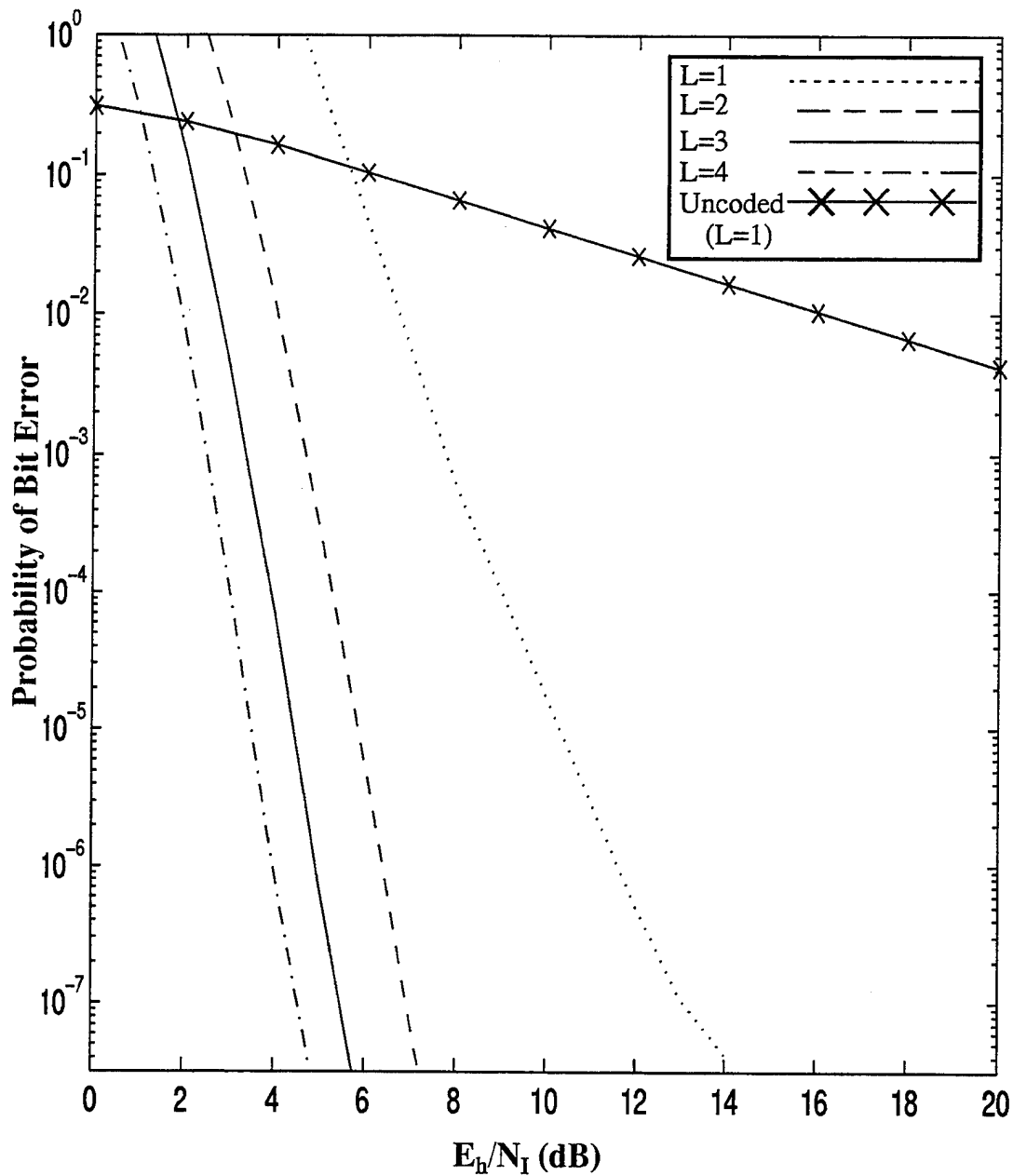


Figure 6.14: Performance of the self-normalized receiver with worst case partial-band jamming, Rician fading and strong direct signal,  $\alpha^2/2\sigma^2=10$ , with  $E_b/N_o=20$  dB,  $L=1,2,3$  and 4 and soft decision Viterbi decoding with  $r=1/2$  and constraint length 7 under assumption of constant energy per hop and varying spread bandwidth.

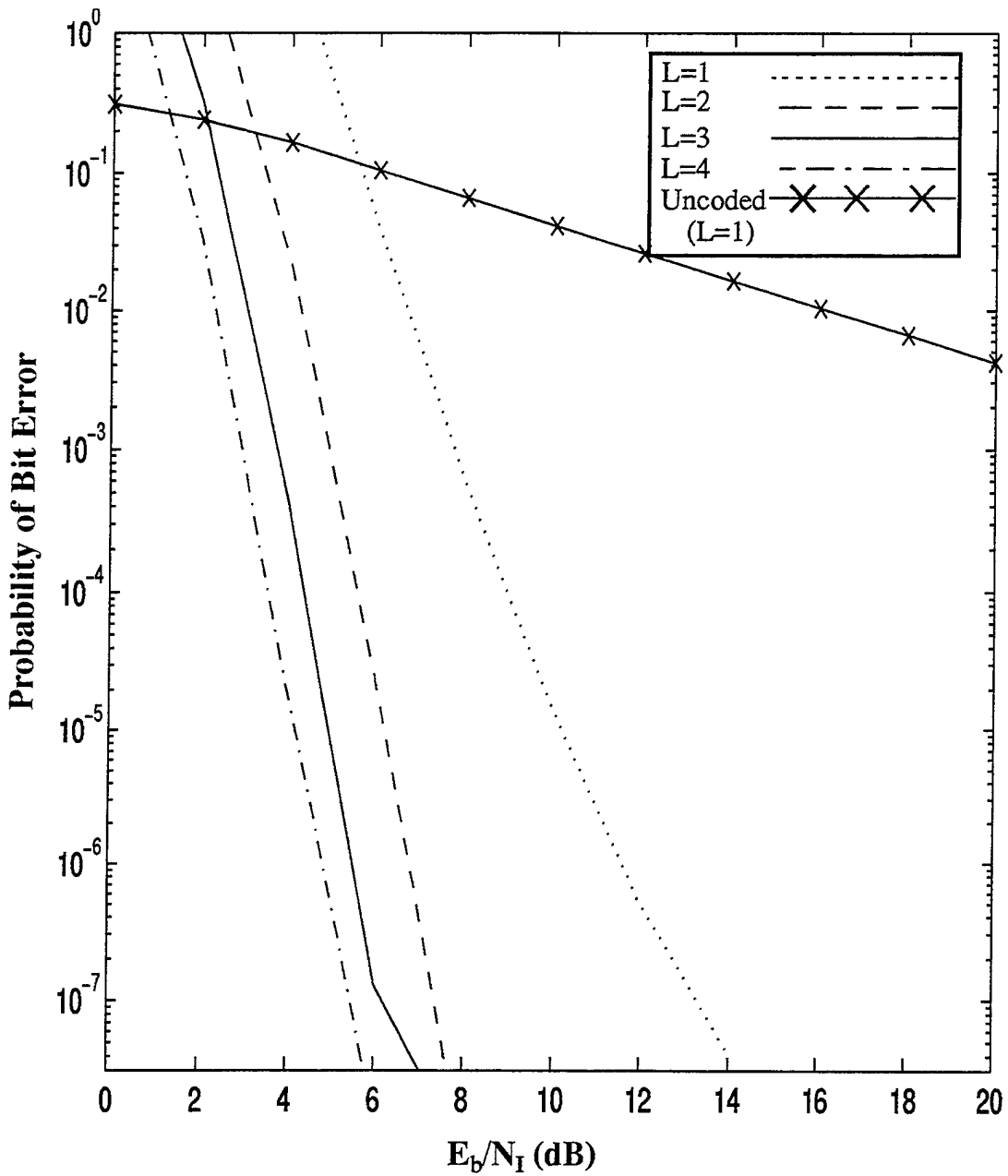


Figure 6.15: Performance of the self-normalized receiver with worst case partial band jamming, Rician fading and strong direct signal,  $\alpha^2/2\sigma^2 = 10$ , with  $E_b/N_0 = 20$  dB,  $L=1,2,3$  and 4 and soft decision Viterbi decoding with  $r=1/2$  and constraint length 7 under assumption of constant energy per bit and varying spread bandwidth.

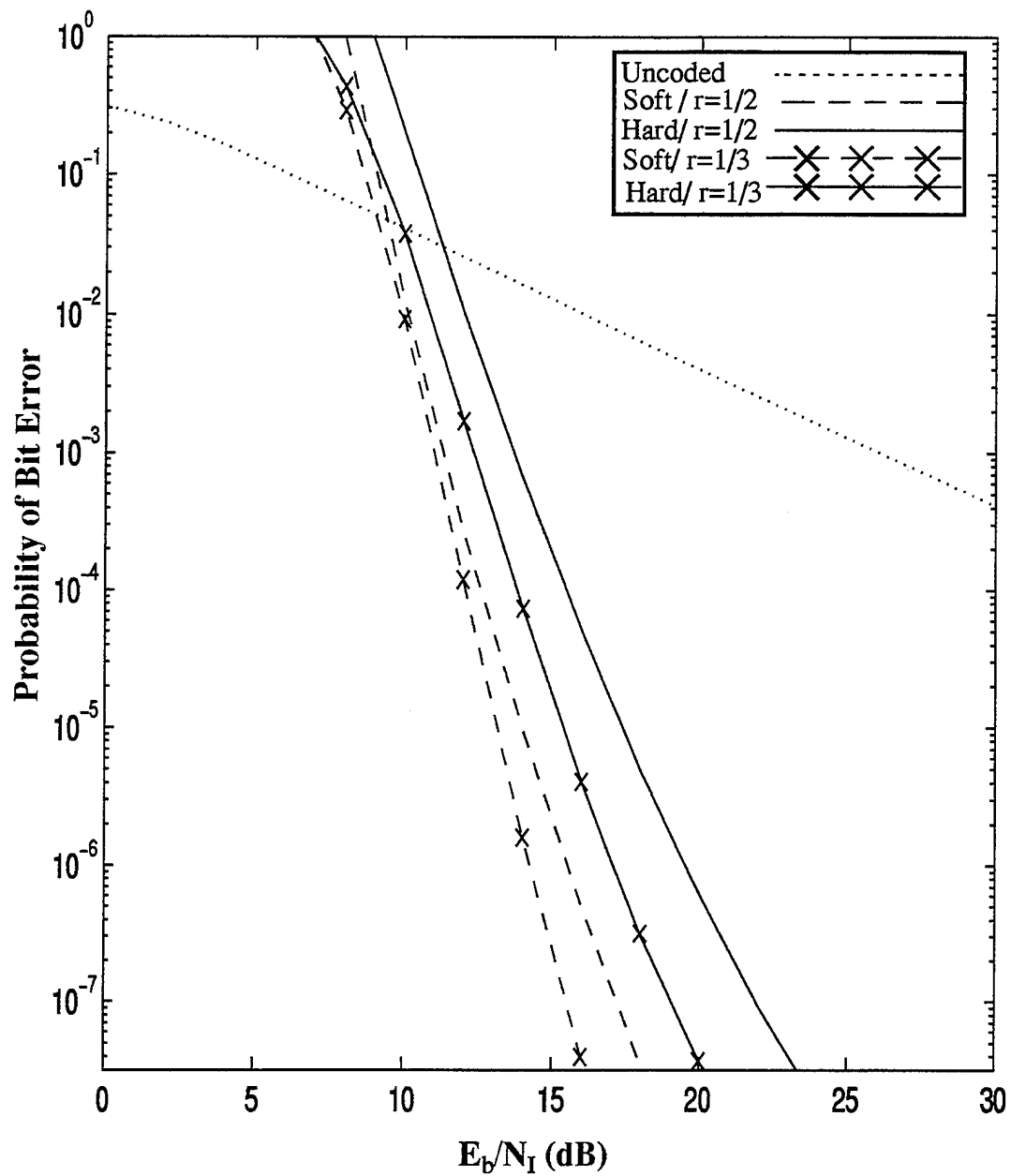


Figure 6.16: Performance of the self-normalized receiver with worst case partial-band jamming, no fading, with  $E_b/N_0 = 13.35$  dB,  $L=1$ , with hard and soft decision Viterbi decoding with  $r=1/2$  and  $1/3$  and constraint length 7.

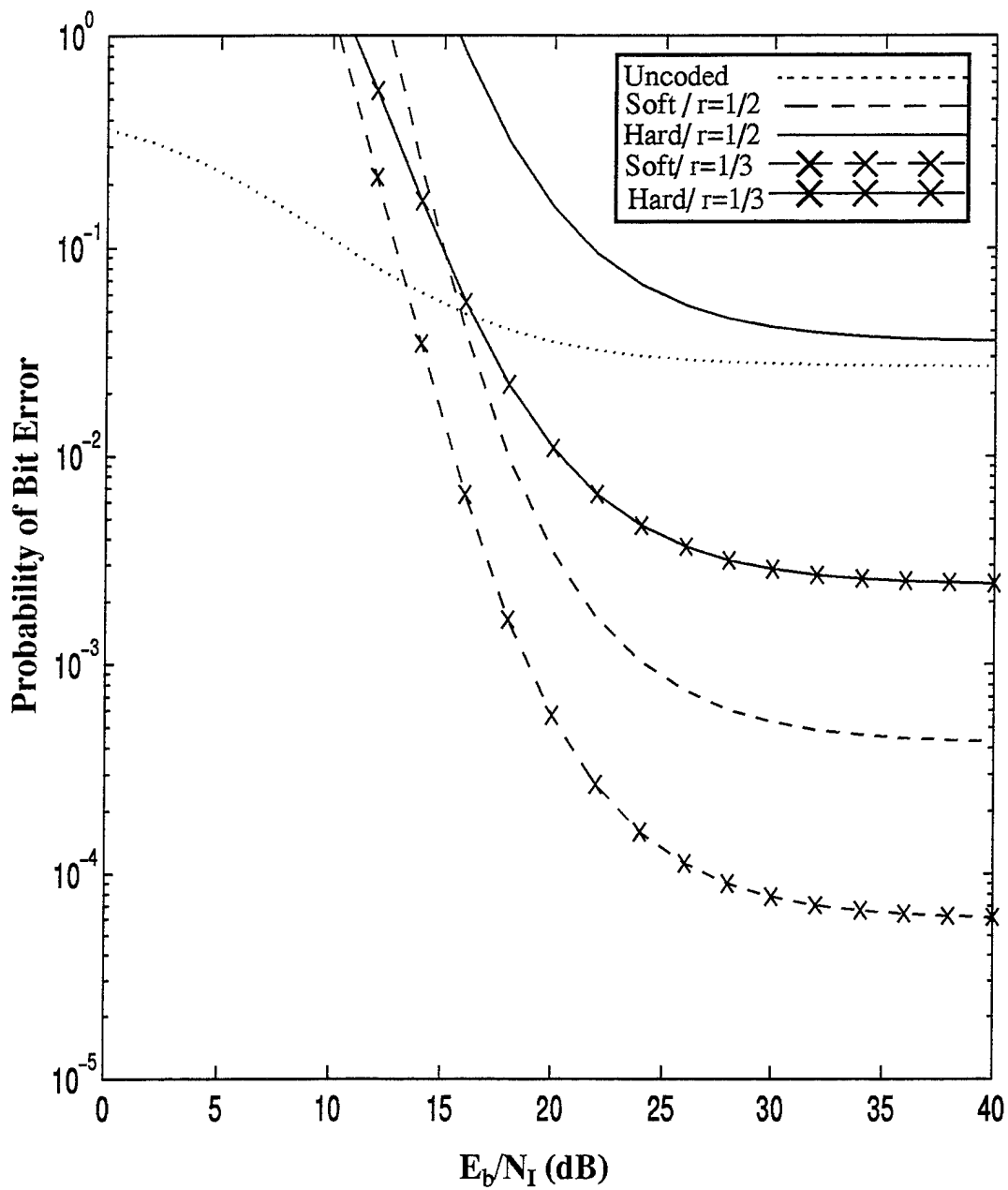


Figure 6.17 Performance of the self-normalized receiver with worst case partial-band jamming, Rayleigh fading, with  $E_b/N_0=13.35$  dB,  $L=2$ , with hard and soft decision Viterbi decoding with  $r=1/2$  and  $1/3$  and constraint length 7.

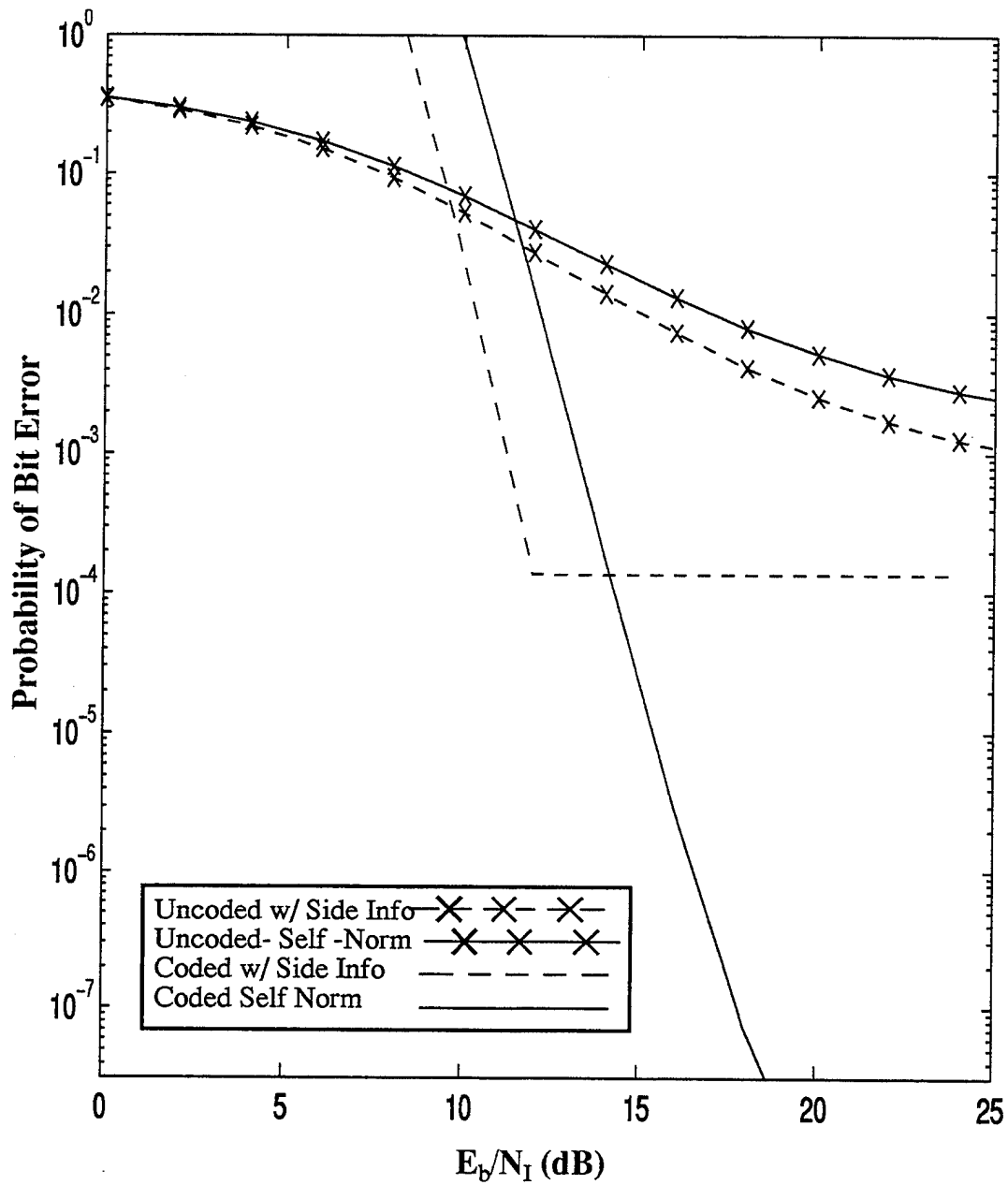


Figure 6.18: Performance of the self-normalized receiver and conventional receiver with perfect side for case of worst case partial-band jamming, Ricean fading with weak direct signal  $\alpha^2/2\sigma^2=1$ ,  $E_b/N_0=13.35$  dB,  $L=2$ , soft decision Viterbi decoding with  $r=1/2$  and constraint length 7.

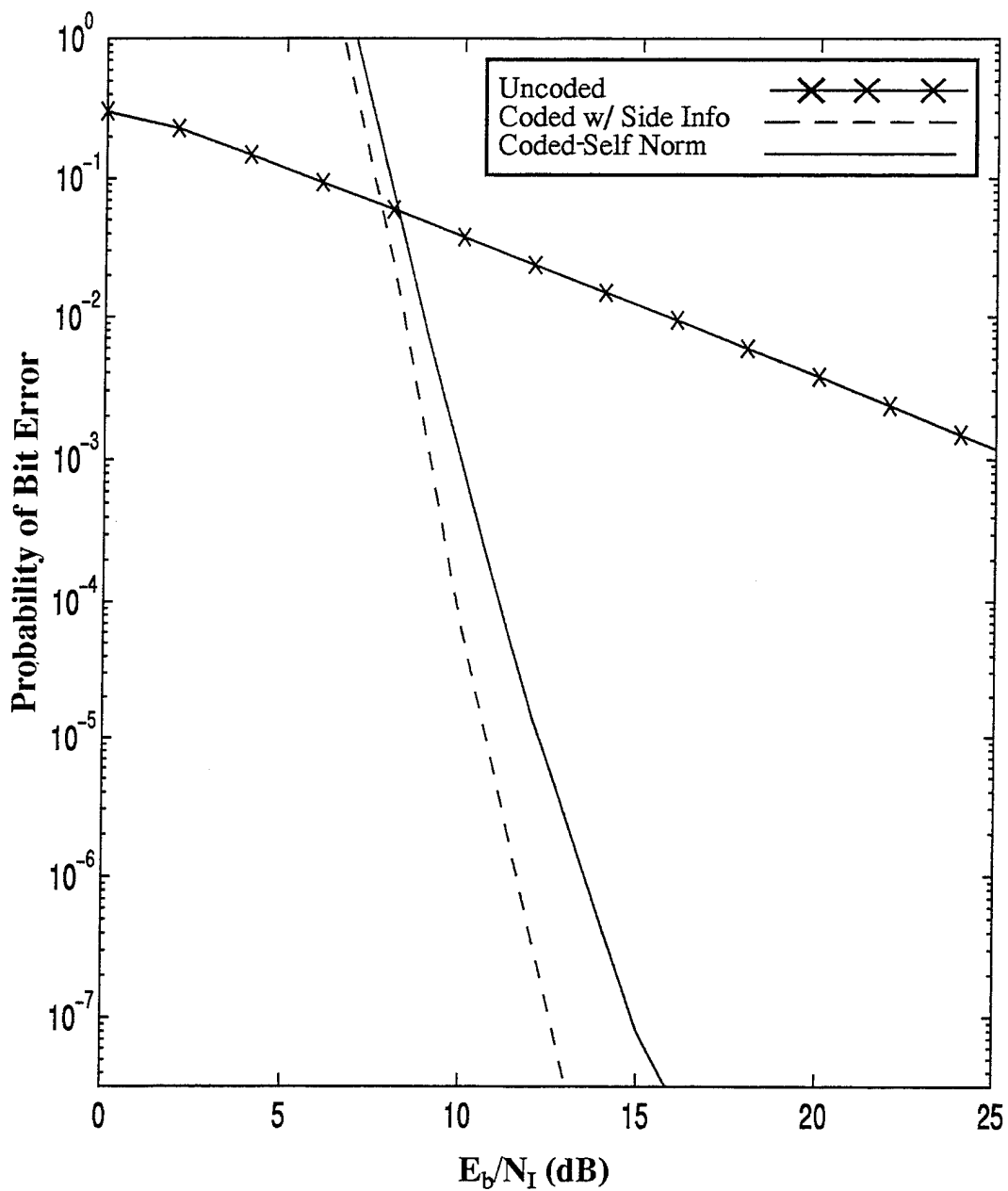


Figure 6.19: Performance of the self-normalized receiver and conventional receiver with perfect side information for case of worst case partial-band jamming and no fading,  $E_b/N_0 = 20$  dB,  $L=1$ , with soft decision Viterbi decoding with  $r=1/2$  and constraint length 7.

## VII. CONCLUSION

Convolutional coding with soft decision Viterbi decoding can dramatically improve the performance of the self-normalized receiver using FFH/BFSK if the uncoded performance is not already too degraded for coding to be effective. When a constant bit energy,  $E_b$ , and constant spread bandwidth is assumed, a coded system with no diversity is superior to an uncoded system with no diversity at moderate  $E_b/N_f$  (above 15 dB for a Rayleigh channel and above 8 dB for a nonfading channel) and when  $E_b/N_o$  is at 13.35 dB. When  $E_b/N_f$  is below these levels uncoded performance is superior. Convolutional coding with soft decision Viterbi decoding forces the jammer towards a full band jamming strategy to cause worst case receiver performance. The use of a more powerful convolutional code (higher constraint length) improves receiver performance and gradually decreases the effectiveness of partial-band jamming over barrage jamming. The difference in effectiveness of partial-band jamming over barrage jamming is dependent upon the degree of fading on the channel and also upon  $E_b/N_o$ . For higher  $E_b/N_o$ , concentrating the jammer power over only a fraction of the bandwidth may be necessary since the signal is not degraded by thermal noise. For a moderate  $E_b/N_o$  of 13.35 dB and a nonfading channel, partial-band jamming is most effective while for a Rayleigh fading channel, barrage jamming is worst case. When  $\alpha^2/2\sigma^2$  is less than 10 and the self-normalized receiver has no diversity, the use of convolutional coding totally defeats partial-band jamming. When a very strong direct signal or no fading exists, convolutional coding mitigates the effects of partial-band jamming, but partial-band jamming is still slightly more effective than is barrage jamming. Totally defeating the partial-band jammer when channel fading is slight requires a more powerful convolutional code than a  $r=1/2, v=9$  code.

For a constant  $E_b$  and  $W$  and  $E_b/N_o$  equal to 13.35 dB, the effect of increasing diversity on performance is again dependent on the degree of fading on the channel. When the system employs convolutional coding with soft decision decoding, performance

degrades slightly when diversity is increased, the received signal is at a moderate  $E_b/N_I$ , and  $\alpha^2/2\sigma^2$  is greater than or equal to 10. Noncoherent combining losses increase with diversity and begin to dominate over the benefits provided by the weighting strategy. This degradation in performance with diversity is in contrast with the uncoded case where the use of diversity improves performance. For a channel subject to severe fading, some diversity is still necessary to improve the performance of a system employing convolutional coding. For a Rayleigh faded channel or a weak direct signal, the use of a diversity of 2 improves performance over no diversity. Diversity levels of 2,3 and 4 all provided similar performance.

Another way to compare the effects of coding and diversity is to allow the spread bandwidth to expand instead of holding it constant. Previous works have typically constrained the spread bandwidth by decreasing the number of hopping frequencies as diversity is increased and coding is added to the system [Ref. 22]. Allowing the spread bandwidth to increase with coding and diversity causes the jammer to spread its available power over a much larger bandwidth. In this case, the use of diversity will improve performance at moderate  $E_b/N_o$  regardless of fading. When the effect of thermal noise is minimal ( $E_b/N_o > 20$  dB), the use of diversity offers all the advantages of a constant energy per hop system without the disadvantage of a decreasing data rate.

Soft decision decoding provides significant benefits over hard decision decoding in a channel with partial-band jamming. The side information provided by the self-normalized receiver is fully utilized by the decoder using soft decisions. The self-normalized receiver without diversity offers no advantage over a conventional receiver when a hard decision decoder is used.

When the jammer interference is greater than thermal noise interference, the coded performance of a conventional receiver with perfect side-information provides only a 1-2 dB gain over the coded performance of the self-normalized receiver. The self-normalized

receiver is superior to a conventional receiver with perfect side information when the relative jammer power decreases and thermal noise effects become more prevalent.

Future extensions of this research should investigate methods to improve the performance of the system to combat the effects of partial-band jamming. Such methods include increasing the modulation orders to greater than 2. The use of increased modulation orders was shown to improve the performance of the noise-normalized receiver and can be assumed to provide similar benefits for the self-normalized receiver [Ref. 3]. Also, further research should be focused towards developing computer models of the system for use in simulations to test the accuracy of the theoretical bit error performance of the system.



## LIST OF REFERENCES

1. Lee, J. S., French R.H., and Miller L.E., "Probability of Error Analysis of a BFSK Frequency-Hopping System with Diversity Under Partial-Band Jamming Interference - Part I: Performance of Square-Law Linear Combining Soft Decision Receiver," *IEEE Trans. Commun.*, vol. COM-32, no. 6, pp. 645-653, June 1984.
2. Lee, J. S., Miller, L.E., and Kim, Y.E., "Probability of Error Analysis of a BFSK Frequency-Hopping System with Diversity Under Partial-Band Jamming Interference - Part II: Performance of Square-Law Nonlinear Combining Soft Decision Receivers," *IEEE Trans. Commun.*, vol. COM-32, no. 12, pp. 1243-1250, July 1986.
3. Robertson, R.C. and Ha, T.T., "Error Probabilities of Fast Frequency-Hopped MFSK with Noise -Normalization Combining in a Fading Channel with Partial-Band Interference," *IEEE Trans. Commun.*, vol. 40, no. 2, pp. 404-412, February 1992.
4. Miller, L.E., Lee, J. S., and Kadrichu, A. P., "Probability of Error Analysis of a BFSK Frequency-Hopping System with Diversity Under Partial-Band Jamming Interference - Part III: Performance of a Square-Law Self-Normalizing Soft Decision Receiver," *IEEE Trans. Commun.*, vol. COM-34, no. 7, pp. 669-675, July 1986.
5. Robertson, R.C. and Ha, T.T., "Error Probabilities of Fast Frequency-Hopped FSK with Self-Normalization Combining in a Fading Channel with Partial-Band Interference," *IEEE J. Select. Areas Commun.*, vol. 10, no. 4, pp. 714-723, May 1992.
6. Peterson, R.L., Ziemer, R.E., and Borth, D.E., *Introduction to Spread Spectrum Communication*, Prentice Hall, Englewood Cliffs, NJ, 1995.
7. H.H. Ma and M.A. Poole, "Error Correcting Codes Against the Worst Case Partial Band Jammer," *IEEE Trans. Commun.*, vol. COM-32, no. 2, pp. 124-133, February 1986.
8. Stark, W.E., "Coding for Frequency-Hopped Spread Spectrum Communications with Partial Band Interference: Part II. Coded Performance," *IEEE Trans. Commun.*, vol. COM-33, no. 2, pp. 1045-1057, October 1985.
9. Chua, A.Y.P., "Error Probabilities of FFH/BFSK with Noise Normalization and Soft Decision Viterbi Decoding in a Fading Channel with Partial-Band Jamming," Master's Thesis, Naval Postgraduate School, Monterey, CA, March 1994.

10. Cheun K. and Stark W.E., "Performance of Robust Metrics with Convolutional Coding and Diversity in FHSS Systems under Partial-Band Noise Jamming," *IEEE Trans. Commun.*, vol. 41, no. 1, pp. 200-209, January 1993.
11. Proakis, J.G., *Digital Communications*, 2nd ed., McGraw-Hill, Inc., New York, NY, 1989.
12. Lam, A.W. and Tantaratana, S., *Theory and Applications of Spread-Spectrum Systems: A Self-Study Course*, class text from EC4500, Naval Postgraduate School, Monterey, CA, 1994.
13. Robertson R.C., "Communication Systems," class notes from EC 4560, Naval Postgraduate School, Monterey, CA.
14. Whalen, A. D., *Detection of Signals in Noise*, Academic Press, Inc., New York, NY, 1971.
15. Clark G.C. and Cain J.B., *Error Correction Coding for Digital Communications*, Plenum, New York, NY, 1981.
16. Lindsey, W.C., "Error Probabilities for Rician Fading Multichannel Reception of Binary and N-ary Signals," *IEEE Trans. Inform. Theory*, vol. IT-10, pp. 339-350, Oct. 1964.
17. McGillem C.D. and Cooper G.R., *Continuous and Discrete Signal and System Analysis, Second Edition*, CBS College, New York, NY, 1984.
18. Beyer William H., *CRC Standard Mathematical Tables and Formaula, 29th Edition*.
19. Gradshteyn, I.S. and Ryzhik, I.M., *Table of Integrals, Series, and Products, Fifth Edition.*, Academic Press, Inc., New York, NY, 1994.
20. Brigham, E. O., *The Fast Fourier Transform*, Prentice-Hall, Inc, Englewood Cliffs, NJ, 1974.
21. Davis, P.J. and Rabinowitz, P., *Methods of Numerical Integration*, 2nd ed., Academic Press, Inc., Orlando, FL, 1984.
22. Simon, M.K., Omura, J.K, Scholtz, R.A. and Levitt, B.K., *Spread Spectrum Communications Handbook*, McGraw-Hill, Inc., New York, NY, 1994.

## INITIAL DISTRIBUTION LIST

1. Defense Technical Information Center 2  
8725 John J. Kingman Rd., STE 0944  
Ft. Belvoir, VA 22060-6218
2. Dudley Knox Library, Code 13 2  
Naval Postgraduate School  
Monterey, CA 93943-5101
3. Chairman, Code EC 1  
Department of Electrical and Computer Engineering  
Naval Postgraduate School  
Monterey, CA 93943-5121
4. Prof. R. Clark Robertson, Code EC/Rc 2  
Department of Electrical and Computer Engineering  
Naval Postgraduate School  
Monterey, CA 93943-5121
5. Prof. Ralph Hippenstiel, Code EC/Hi 1  
Department of Electrical and Computer Engineering  
Naval Postgraduate School  
Monterey, CA 93943-5121
6. U.S. Army Research Laboratory 2  
Survivability/Lethality Analysis Directorate  
ATTN: AMSRL-SL-E (CPT Michael D Theodoss)  
White Sands Missile Range, NM 88002